

Understanding the 5G-air-simulator: a Tutorial on Design Criteria, Technical Components, and Reference Use Cases

Sergio Martiradonna^{a,b}, Alessandro Grassi^{a,b}, Giuseppe Piro^{a,b,*} and Gennaro Boggia^{a,b}

^aDept. of Electrical and Information Engineering - Politecnico di Bari, Bari, Italy

^bCNIT, Consorzio Nazionale Interuniversitario per le Telecomunicazioni

ARTICLE INFO

Keywords:

5G

System-Level Simulation

Performance Evaluation

ABSTRACT


The 5G air interface, also known as New Radio, is providing a significant transformation in the mobile network landscape. It introduces flexible and heterogeneous capabilities to harmoniously blend numerous technical components since a variety of advanced services are being developed, each one entailing different requirements. Nonetheless, the effective management of such a broad diversity is a challenging task to accomplish. As is well known, computer simulation always supported the design, the evaluation, and the optimization of emerging communication technologies, while guaranteeing faster and cheaper investigations than real-world prototypes. This approach is even more useful when applied to the investigation of conventional and extended facilities of the New Radio. The 5G-air-simulator provides a significant step forward in this direction: developed as an open-source system-level tool, it models the key elements of the New Radio (including massive Multiple Input Multiple Output, extended multicast and broadcast, predictor antennas, enhanced random access procedure, NB-IoT) and supports the performance analysis of reference 5G scenarios with different mobility, traffic load, and deployment configurations. This tutorial thoroughly describes both the inner simulator workings and its general-purpose features, while guiding the reader through a series of simulation campaigns for typical 5G scenarios, recently investigated in scientific literature and European projects. Moreover, for each use case taken into account, it deeply explains the syntax used to perform the simulations, the steps to extract the main KPIs, and reference results confirming what presented by the research in this area. The whole contribution, indeed, ensures an immediate usage of the developed simulator for both Academia and Industry, while presenting a calibrated instrument for evaluating the design and the integration of new technical components for current and upcoming mobile radio interfaces.

1. Introduction

The 5th Generation (5G) of mobile networks is going to provide a major shift in the cellular communications landscape. It aims, in fact, at supporting an extreme variety of services, each one with different priorities and performance requirements. For instance, Enhanced Mobile Broadband (eMBB) and Broadcast/Multicast Services (BMS) require high throughput and spectral efficiency, Vehicular to Everything (V2X) needs high mobility and low latency, and Machine-Type Communication (MTC) have to guarantee extensive battery life (and many more examples are possible) [1, 2]. To cope with such broad diversity, many technical components and communication strategies are jointly integrated within a flexible and heterogeneous 5G radio interface [3].

Needless to say, system-level simulation always supported both the design and the evaluation, as well as the optimization of emerging technologies, while guaranteeing faster and cheaper investigations than real-world prototypes. This is even more true for the 5G air interface, i.e. New Radio (NR), where the integration of different components makes the overall system configuration a very challenging goal to accomplish. At the time of this writing, there exist many interesting simulation tools modeling the 5G air interface [4–13]. However, to the best of authors' knowledge, they only implement specific subsets of technical components. Some of them also come with a commercial license, which generally restricts their adoption in many research teams. In parallel with these initiatives, the research group belonging to the Telematics Lab of the Polytechnic University of Bari developed an open-source simulation framework for the 5G air interface, namely *5G-air-simulator* [14]. It intends to overcome the limitations characterizing the aforementioned tools, hence emerging as a valid instrument to study a number of technical components already standardized by the 3rd Generation Partnership Project (3GPP), under investigation by other standardization entities, or recently discussed in the scientific literature [15].

*Corresponding author

 giuseppe.piro@poliba.it (G. Piro)

5G-air-simulator is written in the C++ language, exploiting event-driven and object-oriented paradigms. The source code is readily available at [16]. The developed simulation framework inherits the core functionalities from the worldwide known LTE-Sim tool (including, for instance, the object-oriented and event-driven paradigms, the possibility to simulate, from the system-level perspective, multi-user, multi-cell and heterogeneous network environments, and the implementation of control and data planes with sophisticated and standard-compliant radio resource management methodologies) [17, 18]. Furthermore, it significantly extends the aforementioned project by integrating additional features and many new technical components, which are more suitable for 5G, including:

- New models for channel propagation and data transmission (e.g., Hybrid Automatic Repeat reQuest (HARQ)). Specifically, *5G-air-simulator* has calibrated channel models, i.e., the outcomes of specific simulations [19] are close to those of other similar products considering the same scenario.
- Multiple-Input Multiple-Output (MIMO) and Massive MIMO transmission modes [20]: MIMO techniques are well-established as an important means to increase throughput and spectral efficiency in wireless networks, and Massive MIMO represent an important additional step in this direction.
- Extended multicast and broadcast operation [21]: these paradigms allow many users to receive the same data at the same time and using the same radio resources, avoiding the need to establish multiple individual links, thus saving radio resources and increasing the cell throughput.
- Predictor antennas [22]: fast-moving vehicles usually experience a degraded Quality of Service due to the rapidly changing radio environment, but intelligent use of an antenna array allows the mitigation of this kind of problems while ensuring a greater throughput.
- Enhanced random access procedure [23]: it is present in all mobile protocols, but it is important to study its behavior in 5G due to the potentially massive number of connected devices in MTC.
- NarrowBand IoT (NB-IoT) operation [24]: it is a new air interface designed to serve Internet of Things (IoT) devices with high coverage and low power consumption, while tightly coexisting with other radio technologies.

As a consequence, *5G-air-simulator* may be used to study standalone 5G, as well as LTE-A and NB-IoT deployments.

This tutorial paper provides a detailed description of both the inner simulator workings and its general-purpose features, and it guides the reader through a series of simulation campaigns for typical 5G scenarios. For each of the aforementioned functionalities, it provides a theoretical description of the related technical components, main implementation details, the syntax used to perform the simulations, the steps to extract major Key Performance Indicators (KPIs), as well as the description of example use cases and related reference results confirming what has been presented in the scientific literature. Note that, the simulator already proved to be a valuable tool for different research activities, e.g., the FANTASTIC-5G EU H2020 project [3] and scientific contributions [25–29].

In conclusion, since the simulation platform is freely accessible to everyone, it allows both Academia and Industry to use a calibrated instrument for evaluating the design and the integration of new technical components for current and upcoming mobile radio interfaces. Moreover, given the open-source nature of the tool and its modularity, many new technical components may be integrated in order to pave the way for emerging research directions, such as cellular-connected drones, Network Slicing, etc.

The rest of this tutorial is organized as follows: Section 2 first provides an overview of the main use cases planned or expected in 5G and then describes the 5G Radio Access Network as defined by 3GPP. Section 3 presents a comparison of the 5G system-level simulation tools, while Section 4 describes the structure and the general-purpose features of the new *5G-air-simulator* tool. The remaining sections explore more advanced features specifically developed for some challenging 5G scenarios. In particular, Section 5 describes how the Massive MIMO technology can be used to provide high-bandwidth internet connection in a variety of environments, from rural to urban areas. Section 6 shows how extended multicast and broadcast techniques can be used to realize video streaming for a large number of users in a highly bandwidth-efficient way. In Section 7, the problem of degraded performance on very high-speed trains is presented, and the predictor antenna concept is used to improve the issue to a large extent. Section 8 explains the implementation of an enhanced random access procedure, which is important to improve the performance of massive IoT deployments on cellular networks. Section 9 presents the integration into the simulator of the NB-IoT technology, which is specifically conceived for low-power MTC devices deployed in large numbers. Finally, Section 10 briefly discuss the results of the performance testing of *5G-air-simulator*, whereas, Section 11 outlines the future of the simulator and suggests possible research fields that could take advantage of it. Section 12 concludes the paper.

Table 1

Relation Between 5G Services, Primary KPIs, and Technical Components available in the *5G-air-simulator*.

Service		eMBB	BMS	V2X	mMTC
Primary KPIs	Throughput	✓		✓	
	Coverage	✓	✓		✓
	Mobility			✓	
	Latency			✓	
	Reliability			✓	
	Connection Density		✓		✓
	Energy Efficiency				✓
Technical Components available in <i>5G-air-simulator</i>		Joint Spatial Division Multiplexing, massive MIMO, Interference Coordination (see Section 5)	Multicast-Broadcast Single-Frequency Network, Adaptive Modulation and Coding, Hybrid Automatic Repeat reQuest (see Section 6)	Channel State Information, Separate Receive and Training Antennas with Polynomial Interpolation, Predictor Antennas (see Section 7)	Random Access Protocols, NB-IoT (see Section 8 and Section 9)
Reference 3GPP NR features modeled in <i>5G-air-simulator</i>		Massive MIMO, Adaptive Modulation and Coding, HARQ, Flexible Numerology, Channel State Information		Massive MIMO, Adaptive Modulation and Coding, HARQ, Flexible Numerology, Channel State Information, Dynamic Time Division Duplexing	Adaptive Modulation and Coding, Flexible Numerology, Random Access Procedure

2. Overview of 5G Services and 3GPP New Radio

There are many important differences between 4th Generation (4G) Long Term Evolution (LTE) and 5G. Probably, the most important one lies in the expected set of use cases, which motivates the corresponding design criteria and performance requirements. In the case of 4G, data traffic was expected to be mostly human-driven [30], with some degree of differentiation among flows, e.g. streaming, file transfer, Voice over IP (VoIP). However, the key performance metrics were similar: throughput, delay, spectral efficiency. This fundamental similarity inspired a one-size-fits-all approach for the radio access network, which is designed to support as much of these requirements as possible.

Conversely, the 5G also deals with many data flows that do not involve any direct human intervention, such as IoT devices and connected vehicles [31]. These may have very different requirements from one another, and also with respect to 4G. Moreover, even human-based data exchange could have radically different requirements compared to LTE. This is the case, for instance, with virtual reality, where extremely low latency and reduced jitter are definitely more important than maximizing the throughput [32]. Due to this extreme variation of the requirements, it is not possible anymore to support everything with a single solution. For this reason, 5G does not have a single air interface, but rather a family of air interfaces dedicated to specific use cases, all plugged into a common framework [33]. Moreover, to handle future and unanticipated use cases, it is being designed with flexibility and extensibility at its core. In order to give a general idea of the aforementioned requirements' heterogeneity, the rest of this section will first describe some of the main use cases and the corresponding KPIs, and then it will briefly explain the evolution from 4G to 5G, focusing on the essential 5G air interface features as standardized by 3GPP.

For easier consultation, the primary KPIs for each use case are also listed in Table 1, although it is important to emphasize that they may vary depending on the specific applications. Furthermore, Table 1 also presents the main technical components available in *5G-air-simulator* for enabling the investigated use cases, as well as the standardized features being supported.

2.1. enhanced Mobile Broadband

eMBB generally refers to use cases related to human-based Internet activity that are already common in 4G networks. It embodies practices such as streaming videos, downloading files, browsing the web, performing VoIP or video calls [34]. In most cases, there is a need to download large amounts of data to perform a task. Sometimes, instead, large files need to be uploaded online, e.g., for cloud storage. Either way, the most critical performance metric for the end-user is the perceived connection speed because if it is too low, any operation will take long, hence reducing the user experience. Therefore, the connection speed should be as high as possible, and should also remain sufficiently high for a long time and in extended areas, to give a sense of reliability. Besides, from the operator's perspective, it is crucial to offer the service to as many users as possible. This means that the aggregated throughput supported in a given area should be notably high. The most effective way to reach this goal is to make efficient use of the available resources, e.g., by maximizing spectral efficiency. According to some estimates for the coming years, the user data rates required for satisfactory user experiences are in the range 50-100 Mbps, which translates to a traffic density of tens of Gbps/km² and a spectral efficiency of hundreds of bps/Hz [35].

Massive MIMO emerged as a promising technology able to significantly improve the performance in terms of spectral efficiency and reliability [36]. Indeed, by utilizing a massive number of antennas at the base station, the information data may be multiplexed on each radio resource, concentrating the radiated energy toward the intended directions while minimizing the interferences. For reaching these ambitious targets, the implementation of Massive MIMO in the developed 5G network simulator is presented in Section 5.

2.2. Broadcast/Multicast Services

Even though communications are increasingly becoming personalized, there are additional cases where either one-to-many or one-to-all distribution model is appropriate. Moreover, the wireless medium is naturally a shared one, and multicast/broadcast schemes are the best way to take advantage of this feature [37]. Notable applications of this idea include video broadcasting in social events such as concerts and sports matches, local emergency warnings for dangerous weather conditions, and large-scale firmware updates for IoT or automotive devices [38].

The main objective for these scenarios is to achieve extensive and consistent coverage. However, this has to be balanced with throughput, since a higher transmission rate (achieved via higher modulation orders and code rates) makes the reception more challenging for cell-edge users. When multiple cells are involved, they need to be tightly synchronized, and managing multiple partially-overlapping broadcast areas may become difficult. Moreover, the network should have means to detect the presence of users interested in the same content, to decide whether a multicast transmission is appropriate, and to establish it on-the-fly. This is clearly reflected in the fact that LTE has supported a usable broadcasting feature since Release-9, that is the Multicast Broadcast Single Frequency Network (MBSFN) [19]. Although 3GPP Release 15 only supports unicast delivery, work is on-going in Release 16 and the introduction of multicast/broadcast in 5G NR is expected to start in Release 17 for offering new opportunities beyond the capabilities of the previous generation mobile broadcasting [39]. As a consequence, in Section 6 the MBSFN technique of LTE is used as a starting point, and extensions based on the use of a feedback channel are built on top of it.

2.3. Vehicular to Everything

V2X refers to scenarios where moving vehicles are involved [40]. In this field, numerous exciting applications are possible. One of them is infotainment, where an Internet connection is utilized to provide both entertainment content for passengers and valuable information for the driver, such as traffic and weather forecasts [41]. The technical requirements would be similar to the eMBB use cases, with the added complication of mobility and possible signal drops. Assisted and autonomous driving, where the vehicle can autonomously perform some maneuvers or adjustments, based on available information about the immediate surrounding, is a different application [42]. In this case, the fundamental features of the underlying communication system are reliability and low latency, to enable timely responses from the assisted driving unit [43]. Section 7 presents the scenario of very high-speed trains, which is yet another V2X application, where broadband performance is impaired and shows the use of predictor antennas as a possible solution.

2.4. massive Machine Type Communications

The IoT is growing steadily, approaching 11 billion devices [44]. Communications involving these connected objects are usually referred to as MTC, but since their number is so high (and growing), this use case is often called Massive Machine-Type Communications (mMTC). Using cellular networks is an attractive option to provide IoT devices with Internet connectivity, because of their widespread deployment and reliable operation. However, current

networks are not entirely suited for this use, as they mainly focus on throughput and spectral efficiency. Instead, connected things have different needs.

The majority of these devices are sensors that periodically make measurements and send data to a server, so transmission is largely uplink-dominated. They also need to operate from a battery for a very long time, up to 10 years, because replacing batteries frequently for so many devices is expensive (especially in terms of human work) and inconvenient. Coverage is also an issue: IoT devices may be placed in hard-to-reach places, such as basements or underground pipes, where cellular signal is weak or missing. To this end, the communication technologies oriented towards IoT applications may need a coverage enhancement, in terms of Maximum Coupling Loss, ranging from 10 to 20 dB, when compared to current networks [45]. Finally, supporting a very large number of devices connected to the same cell may prove difficult, as they may be orders of magnitude more numerous than human users [46].

Section 8 describes an enhanced protocol for the random access channel, which can be a bottleneck for massive deployments of MTC devices. Moreover, Section 9 introduces the NB-IoT technology, which also addresses the other requirements of MTC devices.

2.5. 3GPP NR

The 3GPP is a global standards development organization and has been developing 5G NR over the past few years. The expectation is that 5G NR is a totally new air interface that can operate alongside 4G LTE. However, differently from previous generations, the essential enhancement of 5G with respect to 4G is not only the ability to handle much faster data rates and to provide higher capacity for users. In fact, key NR features include advanced antenna technologies, spectrum flexibility, operation in high frequency bands, dynamic Time Division Duplex (TDD), and support for low latency. In addition, achieving the 5G expectation, it is essential that 5G NR must be able to deliver numerous and varied services across a different set of devices with different performance and latency needs.

It is important to underline that a part of 5G expected capabilities can be provided also on top of recent LTE-Advanced Pro networks. As a matter of fact, 4.5G Pro supports 1 Gbps with carrier aggregation and 4×4 MIMO [47].

2.5.1. Release 15

Release 15 is the first ever 5G-compliant standardization work conducted to produce the initial NR specifications. In this initial NR specification, drafted from the beginning of 2017 to 2019, the target objectives were set to specify the functionalities for eMBB and to lay the cornerstones for providing Ultra Reliable and Low Latency Communications.

NR is the first mobile radio technology that is designed to operate on any frequency band between 450 MHz and 52.6 GHz. The lower bands are needed for coverage, while the higher bands will provide high data rates and capacity. Specifically, 3GPP defines two frequency ranges: the first one (Frequency Range 1) covers the frequencies between 450 MHz and 6 GHz range, whereas the second one (Frequency Range 2) refers to the frequencies within the 24.25–52.600 GHz interval. These frequency ranges are commonly referred to as sub-6 GHz and millimeter-wave, respectively. According to the specifications [48], the initial 5G deployments use TDD between 2.5 and 5.0 GHz, Frequency Division Duplex (FDD) below 2.7 GHz, and TDD at millimeter wave at 24–39 GHz. As it happened with the LTE development, it can be expected that there will be several new 5G operating bands and channel bandwidths in forthcoming 3GPP releases.

After the evaluation of new candidates to 5G waveforms, the Orthogonal Frequency Division Multiplexing (OFDM) was chosen, as its performance has been proven in LTE over the last years. However, it has been further optimized to tackle the strict 5G requirements and enabling lower latency compared to the 4G version. In LTE, OFDM subcarriers have a fixed spacing of 15 kHz, and 12 subcarriers in the frequency domain defines the basic radio resource, namely the Resource Block (RB). Although also in 5G a RB has 12 subcarriers, 3GPP introduces in the NR standard the idea of flexible numerology, characterized by a set of supported subcarrier spacings and cyclic prefixes [49]. Specifically, Release 15 supports spacing equal to 15 (as in LTE), 30, 60, 120, and 240 kHz, i.e., RBs of 180, 360, 720, 1440, and 2880 kHz width, respectively. While all these spacing support the normal cyclic prefix length, only 30 kHz spacing also supports the extended one, thus accounting for a total of 6 different supported numerologies. It is worth mentioning that 240 kHz subcarrier spacing is only used for synch and it does not support data transmission. [50]

In the time domain, NR tries to maintain a certain backward compatibility with LTE. As a consequence, similarly to LTE, the NR frame is 10 ms long, and it is composed of ten subframes of 1 ms each. Nonetheless, according to the chosen numerology, each subframe is split into a variable number of slots, which increases with the subcarrier spacing. In accordance, the slot length is smaller for higher spacings. Each slot then contains a fixed number of OFDM symbols:

14 symbols for the normal cyclic prefix length and 12 for the extended one. This architecture enables a flexible NR frame structure, allowing different number of slots per subframe, as well as varying OFDM symbol and slot lengths.

To address scenarios characterized by rapid per-cell traffic variations, NR defines dynamic TDD, that is the possibility for dynamic assignment of resources between the downlink and the uplink transmission directions. In other words, the number of uplink and downlink slots in a frame may be changed according to the traffic demands of downlink and uplink directions. In addition, the resource scheduler, which is in charge of conduct this dynamic assignment, works on a per-slot basis, instead of the per-subframe basis typical of LTE, hence with a finer grain.

An additional level of flexibility in NR is achieved with the concept of BandWidth Part (BWP), which is a subset of the total bandwidth of a cell. In particular, a user can be configured to support one or multiple BWPs, even though only one can be active. This is done essentially for two main reasons. First, in order to maintain the hardware of the user devices at a reasonable level complexity, since operating bandwidth of NR is much higher compared to LTE (up to 100 MHz and 400 MHz for sub-6 GHz and millimeter-wave, respectively). Second, for multiplexing different numerologies in the frequency domain, in order to support various traffic types with different requirements.

Thanks to many of the features discussed above, Release 15 also supports and assists usage scenarios for mission critical services that require extremely low latency and high reliability. As mentioned earlier, low latency is implemented by using a wide subcarrier spacing and reducing the number of OFDM symbols used for data assignment, e.g., a mini-slot can be used to support these services. With reference to the latter example, NR also defined procedures to enable what is called punctured scheduling in the downlink direction [51]. Specifically, low latency may be achieved by puncturing the resources already assigned to other traffics while informing the affected users, in case of a sudden need for resources by a prioritized flow. On the other hand, to implement high reliability, new modulation and coding schemes are specified to support even lower signal ratios. As a matter of fact, while LTE uses Turbo and convolutional coding, NR adopts Polar Codes for control channels and Low Density Parity Check coding for data channels, which can offer lower complexity, especially at higher code rates, and better performance for small packet sizes. In addition, while LTE can utilize QPSK, 16QAM, and 64QAM modulation schemes, NR may use up to 256QAM, hence increasing throughput and spectral efficiency.

Massive MIMO is another of the key enabling technologies for 5G and it has been part of NR specifications and deployments from the beginning. Differently from the MIMO systems in current 4G standards, Massive MIMO is based on 2D active antenna arrays with a large number of antennas at base stations. This bidimensional structure implies that the radio signal on both vertical and horizontal planes can be controlled simultaneously through a mechanism called 3D beamforming, which can increase spectral efficiency and network coverage substantially. These advancements allows to use coding techniques for significantly mitigating the interference between nodes. Nevertheless, such benefits can only be guaranteed if perfect channel knowledge is available at the base station. For this reason, several design challenges needs to be considered to implement Massive MIMO in practical systems, as deeply discussed in Section 4.2.2 and Section 5. Release 15 supports up to 256 antenna elements on base stations and up to 32 antenna elements on terminals. With this configuration, the downlink supports single user MIMO transmission with up to 8 layers and multi-user MIMO transmission with up to 12 layers, whereas the uplink supports single-user MIMO transmission with up to 4 layers. It is important to note that Massive MIMO and beamforming is assumed throughout the specifications not only for data transmission but also for several other aspects, e.g., reference signal structure, beam management, initial access, scheduling, and HARQ retransmission.

2.5.2. Release 16 and 17

A big part of the focus of Release 16 is addressing more vertical segments with respect to the use case expected by Release 15, e.g., transportation industry, factory automation, and power distribution, hence covering V2X and mMTC. This Release is expected to have specifications frozen in June 2020 [47]. On the one hand, Release 16 will provide several enhancements to already standardized features, like MIMO with Multiple Transmission Point(Multi-TRP) for the provision of high reliability and robustness of connection thanks to the increased diversity, and a two-step RACH, for reducing the delay of the traditional four-message random access operation. On the other hand, it will introduce completely new topics, i.e., Integrated access and Backhaul [52] and NR-Unlicensed (NR-U) [53]. Integrated Access and Backhaul allows part of the radio access spectrum resources to be used for backhaul transmission, hence enabling a cost-effective deployment option, especially in contexts where a fiber infrastructure is lacking. Instead, the possibility offered by enabling 5G operations in unlicensed spectrum with NR-U, allows to achieve coverage extension as well as to support higher bandwidth operation, hence boosting the performance. At the same time, fair coexistence can be ensured with the wireless technologies which have been already deployed in the 5 GHz band, e.g., Wi-Fi and LTE-based

Table 2

Comparison of the features of various 5G system-level simulators.

Feature	[4]	[5]	[6]	[7]	[8]	[9]	Vienna [10]	5G K- SymSys [11]	NetSim [12]	WiSE [13]	<i>5G-air-simulator</i>
Massive MIMO			✓		✓			✓		✓	✓
Multicast/Broadcast											✓
Predictor Antennas											✓
Random Access Procedure						✓		✓			✓
NB-IoT			✓								✓
MIMO				✓	✓	(✓)	✓			✓	✓
HetNet			✓		✓	✓	✓			✓	✓
Calibrated channel models	✓					(✓)		✓		✓	✓
Flexible Numerology					✓	✓	✓	✓	✓	✓	(✓)
mmWaves					✓		✓	✓	✓		
Dual/Multi connectivity				✓	✓	(✓)			✓		
Device-to-Device (D2D)							✓				
Integrated system and link-level		✓					✓				
Integrated network simulator					✓	✓		✓			
General information											
Programming language	N	N	N	U	C++	C++	Matlab	C++	C	C++	C++
License	N	N	N	U	GNU GPL	GNU GPL	Acad.	Acad.	Comm.	Comm.	GNU GPL
Open-source	N	N	N	U	✓	✓	✓	✓			✓
Usable implementation available				✓	✓	✓	✓	✓	✓	✓	✓

Note: * N = N/A, U = Unknown, (✓) = partial implementation of the reference feature.

Licensed Assisted Access.

As for the key directions for Release 17, they will be mainly the work on frequency bands higher than 52.6 GHz and up to 114 GHz, as well as Non-Terrestrial Networks and Coverage Enhancement [54].

3. State of the Art on 5G System-Level Simulators

This tutorial is oriented toward a specific type of simulation, i.e., system-level simulation modeling complete networks with multiple base stations and a large number of mobile users for the evaluation of procedures related to mobility, application, physical transmissions, scheduling, frequency reuse, and so on. To limit complexity to an acceptable level, system-level simulators employ various simplifications. The opposite category is that of link-level simulation, where the models go into great levels of detail, but simulation is usually limited to a single link, hence the name. Link-level simulations are used to investigate topics that can be limited to a single communication link, and the results can be used to construct simpler and faster models to realize system-level tools.

At the time of this writing, some simulators are known to be available or in development for the 5G. A comparison of the main qualities available in them is shown in Table 2, separated into features and general information. It is important to underline that some of the missing features of the *5G-air-simulator* are either part of the future work (as reported in Section 11) or out-of-scope with respect to the main goals of the tool presented herein.

The work in [4] describes a two-level simulator, including the core network and the access network as well as their interactions, which also takes advantage of cloud resources to speed up the simulation. However, this architecture

is only a high-level proposal and there is no actual implementation yet. Similarly, the authors of [5, 6] outline an architecture for 5G simulators, but the simulators themselves are still not complete and only some features are presented in the papers. The simulator presented in [7] seems to be an actual product with various features but is not stated whether it is open source or otherwise available to the public. Moreover, the only relevant feature that falls into the 5G realm is the aggregation of cellular and Wi-Fi traffic, i.e. dual connectivity.

The work [8] presents an open-source simulation tool for LTE-like 5G mmWave cellular networks integrated into the widely used open-source ns-3 simulator [55]. Starting from both this module and the LTE module (LENA) [56], the authors of 5G-LENA [9] conducts a comprehensive and intensive work to align both modules to the latest standard published by 3GPP and build a NR simulator. However, despite its compliance with the latest standards, the number of offered features is rather limited: it lacks spatial user multiplexing, MIMO and Massive MIMO, and FDD.

On the other hand, Vienna 5G system-level simulator [10], which is a direct evolution of the pre-existing LTE-Advanced (LTE-A) system-level simulator, adds many 5G-related capabilities such as new propagation models, heterogeneous networks, D2D operation, relays, and IoT scenarios. Also, the 5G K-SimSys simulator [11], which is part of the 5G K-Simulator platform [57] integrating link, system and network-level simulators, offers several 5G capabilities. While this feature set is remarkable compared to other available simulators, the comparison with our *5G-air-simulator* is not this immediate. In fact, the simulators share some common features, whereas some functionalities are only available in the Vienna and 5G K-SimSys simulators (e.g. D2D, mmWaves) and some are exclusive to *5G-air-simulator* (e.g. Massive MIMO, broadcasting). As for licensing, the Vienna and 5G K-SimSys simulators are freely available for academic purposes, but require the purchase of a license for commercial use, while *5G-air-simulator* is under GPL license, thus it is free to use for everyone and the source is always available.

It is worth noting that [8, 9, 11] are also network simulators, hence allowing not only the analysis of the application and the radio interface layers of but also of end-to-end scenarios with a full protocol stack.

Other simulators can be purchased using a commercial license, therefore their source codes are not publicly available. Specifically, there is the NetSim's 5G library for mmWave networks [12] and the WiSE simulator [13].

In conclusion, *5G-air-simulator* offers many technical components enabling the 5G air interface and calibrated channel models. Moreover, since it is under GPL license, it allows for a simple and fast utilization, as well as the possibility to investigate new protocols and technologies by extending the available code.

4. An Overview of 5G-air-simulator

5G-air-simulator is written in the C++ language with an object-oriented paradigm and extends the popular LTE-sim network tool [17]. The source code is readily available at [16]. To help the reader understand its inner workings and how some features and properties are achieved, this section encompasses some general properties of the *5G-air-simulator*. Figure 1 depicts the main building blocks of the developed tool. Simulator's core represents the first key building block, providing all the procedures useful to implement object-oriented and event-driven paradigms, as well as to manage nodes, protocol stack, mobility, and applications. It mainly inherits from the well-known LTE-Sim tool [17]. On top of the simulator's core, the *5G-air-simulator* integrates many other supporting models that significantly extend the features initially offered by LTE-Sim. They include the calibrated and standard compliant Link-To-System (L2S) model, MIMO features, and HARQ. These latter models offer a suitable substrate for the development of 5G technical components, like Massive MIMO, extended multicast/broadcast transmissions, predictor antennas, enhanced random access procedure, and NB-IoT. Although reference scenarios have been developed to conduct a performance assessment of each 5G technical component almost independently, it is worth mentioning that a simulator's user can realize completely new scenarios (as explained in Section 4.4) by combining multiple components. As a matter of fact, all the presented building blocks may be used concurrently depending on the users' needs. At the time of this writing, however, the NB-IoT component only works standalone. This aspect will be tackled in the future when it will be clearer the inclusion of NB-IoT in 5G NR specifications.

The simulator's core and its supporting models are presented in this Section, while the implemented 5G technical components will be deeply discussed later on.

4.1. Core of 5G-air-simulator

5G-air-simulator is structured as an event-driven application: the `Calendar` class holds a list of events to be executed, with each item containing the required time of execution, the method to execute, the object on which the method should be called, and possibly some parameters. Other important classes are `Simulator` and `Framemanager`.

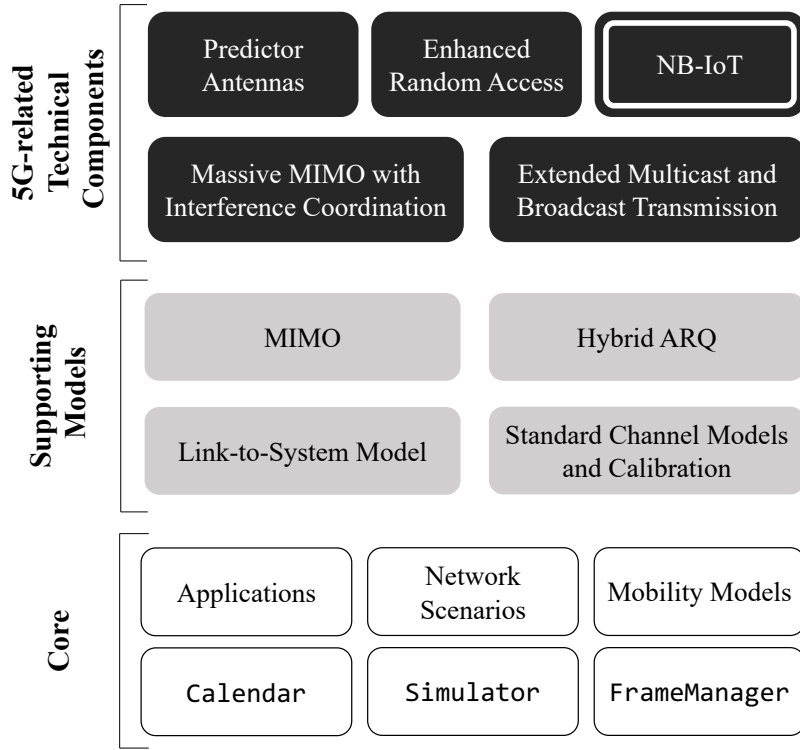


Figure 1: Building blocks of the *5G-air-simulator*. NB-IoT is an independent component built directly on the Core.

Simulator is a singleton class performing global actions, such as initiating and halting the simulation, adding events to the *Calendar*, and running them. The *FrameManager* tracks the flow of time, increases the counters related to frames and sub-frames, and, in some cases, it marks sub-frames dedicated to different functions, e.g., downlink versus uplink sub-frames in TDD mode [58]. Practically, it is in charge of scheduling the events related to the start and the end of frames and sub-frames according to a fixed frame structure.

At the beginning of the program's flow, one of the available scenarios is selected. The scenario is in charge of creating and initializing many important elements of the simulation environment, such as the base stations, mobile terminals, and channel realizations. Most scenarios also accept several parameters that affect the specific details of the objects that are created (e.g. the scheduling algorithm at the base stations [18] or the periodicity channel state reporting) or even the simulation as a whole (e.g. the total duration or the size of the environment). In some cases, the initialization of some objects defines some events that are inserted into the *Calendar* class, to be executed at a later time. This includes, for instance, the generation of data packets at the application layer and the movement of the devices.

After all the initial setup, the actual simulation is started by calling the *Simulator::Start()* method. At this point, the *Calendar* class starts executing the registered events in chronological order. Each event can result in the generation of new events that are put in the calendar, resulting in a sustained supply of events to process until the end of the simulation. In particular, some kinds of events re-schedule themselves just at the end of their execution, thus repeating periodically for the entire simulation time. These include the allocation of radio resources and the reception procedures of each device. The generation and execution of events go on until a call is made to the *Simulator::Stop()* method, which causes the calendar to stop and discard all the events that may still be pending, and finally terminate the program. Usually, the end time of the simulation is set in advance via a call to *Simulator::SetStop()* in the scenario, right before calling *Simulator::Start()*.

4.1.1. Application Layer and the Protocol Stack

In *5G-air-simulator*, application models are in charge of generating data packets that are then forwarded through the protocol stack, transmitted, and then processed at the receiver's protocol stack. Different models are available to cover varying situations. They are all derived from the same `Application` class, thus introducing new models is as simple as writing a new class derived from it.

A straightforward model is the `InfiniteBuffer`. A transmitting node using this model acts as an infinite supply of data: at every occasion for communication, it generates as much data as can be transmitted, for the entire simulation. This model is intended to put as much stress as possible on the network and measure its maximum capacity.

The `TraceBased` model is intended to emulate the traffic generated from video streaming. The model contains many traces created from an actual video file [59], containing the size and timestamp of each frame. These are then used to generate data packets at the appropriate times. If the end of the trace is reached, it is restarted from the beginning.

For voice traffic, there is a `VoIP` model: it follows the G.729 model [60], thus generating packets of constant rate and size, but only during the so-called active state. Instead, in the inactive state, no packets are created. At any given time, there is a given probability of going from active to inactive state or vice-versa, thus reflecting the intermittent nature of human speech.

Web browsing is described with the `FTP2` model [19], where packets of a given size (representing a web page) are generated at random intervals (representing the inactive time where the user is reading). The average duration of the interval is modeled with an exponential probability, where the mean value is given as a parameter, together with the packet size.

Finally, the simplest model is constant bit-rate or CBR. It generates packets of a fixed size at fixed regular intervals, which are both input parameters. This model is intended to represent applications that transmit data with a strict recurring schedule, such as remote sensors producing periodic reports.

5G-air-simulator also supports several other features of both user- and control-plane protocol stacks. To this aim, each device implements an instance of the `ProtocolStack` class, which in turn contains `Media Access Control` (MAC), `Radio Link Control` (RLC), `Packet Data Convergence Protocol` (PDCP), and `Application` entities. The `Application` entity associates the sources with the destinations of each application flow, which is generated as mentioned above. The `PDCP` Entity mainly handles the header compression of all the packets coming from the upper layer and enqueueing into the `MAC` entity. The `RLC` Entity models the three data transfer modes, namely `Transparent Mode` (TM), `Unacknowledged Mode` (UM), and `Acknowledged Mode` (AM), and handles the buffering, segmentation/reassembly, and retransmission of service data units. Each dedicated radio bearer has its own `RLC` entity. The `MAC` Entity provides, for both users and gNBs, an interface between the device and the `PHY` layer, for delivering packets coming from the upper layers to the `PHY` one and vice versa. Furthermore, the `Adaptive Modulation and Coding` (AMC) module and the `Packet Schedulers` also belong to the gNB's `MAC` entity.

At the bottom of the protocol stack, the `Phy` class allows to customize physical characteristics, by setting the transmission power, the number of transmitting and receiving antennas, and the noise figure for both users and base stations. Furthermore, for base stations only, it is also possible to choose between omni-directional or tri-sector antennas. In the latter case, several parameters may be customized, e.g., antenna bearing and its gain, e-tilt, horizontal and vertical beam width at 3 dB, feeder loss, and maximum horizontal and vertical attenuation.

4.1.2. Network Deployments and Mobility Models

5G-air-simulator includes a number of basic scenarios reflecting typical conditions used in research and testing, ranging from a single cell to heterogeneous network configurations, as depicted in Figure 2. The simplest one is called `SingleCell`: as the name suggests, it only contains one cell and a single omnidirectional base station, with a configurable number of users in it. Also, since there are no other cells around, there is no inter-cell interference. This architecture may be used, for instance, to evaluate peak throughput or coverage under ideal conditions or for isolated sites.

A more realistic configuration is constructed in the `SingleCellWithInterference` scenario. There is still a single omnidirectional base station with active users, but this time it is surrounded by other base stations that do not serve any user. Nonetheless, they still create inter-cell interference, modeled as an always-on transmission at full power in all the radio resources. Therefore, these surrounding interfering nodes influence the performance metrics measured in the primary cell.

For more in-depth evaluations, the `MultiCell` scenario creates a full multi-cell environment with multiple active base stations, each with multiple users. With this setup, it is possible to evaluate issues such as frequency reuse and

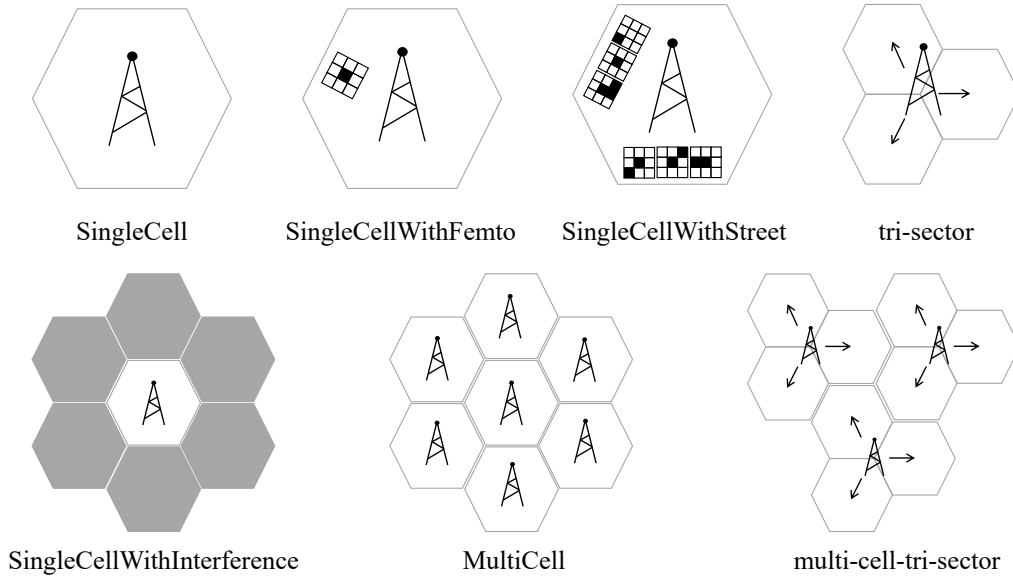


Figure 2: Network deployments available in *5G-air-simulator*.

handover, although the simulation time may increase substantially.

Instead of omnidirectional base station, for some scenarios there are also versions with three-sector cells: *tri-sector* is similar to *SingleCell*, except that there are three co-located base stations and each one serves a 120° wide sector. While there is still no interference from other base station sites, there is still interference among sectors, so it is not as idealized as the *SingleCell* case. Similarly, *multi-cell-tri-sector* is similar to *MultiCell* but with each cell replaced by three 120° sectors. This configuration is the most similar to real-world deployments among those presented here.

Finally, two additional scenarios involve heterogeneous networks [61]. *SingleCellWithFemto* involves a single macro-cell together with many femtocells, deployed into houses belonging to a group of buildings. Some of the users are placed into the coverage area of the cell, while others are created in clusters near the femtocells. Similarly, the *SingleCellWithStreet* scenario constructs a single macro-cell and a configurable number of streets, where each street includes a block of buildings and the corresponding femtocells. These scenarios are intended to investigate issues related to such heterogeneous configurations, such as access policies, handover, and scheduling [62].

5G-air-simulator includes different mobility models [63], and others may be easily implemented. *ConstantPosition* is the most simplistic one, as the users do not move. In *RandomDirection*, users move with a constant speed towards a given direction, that is randomly selected at the beginning of the simulation. When the limit of the simulation area is reached, a new direction is selected (pointing back towards the simulation area) and it is followed until the end of the area is reached again, then the process is repeated. Similarly, the *LinearMovement* model allows selecting a given direction. On the other hand, when using the *RandomWalk* model, users still move toward a random direction, but they do not need to reach the end of the simulation area. Instead, the direction is changed after traveling a certain distance. The last available mobility model is called *Manhattan*: in this case, the user can only move in a horizontal or vertical direction, and at any given time it has a certain probability to turn left or right. This is intended to represent city environments where all the streets are at straight angles.

As reported previously, there is the possibility to implement even more mobility models. For instance, it is possible to implement the well-known *Random Waypoint* as an extension of the baseline *RandomWayPoint* class, which is already available in the code. However, it is necessary to highlight that, at the time of this writing, mobility models do not interact with the possible presence of buildings in scenarios.

Finally, although users arrivals and departures are not modeled, i.e., the number of users is fixed throughout an entire simulation, it is possible to model the arrivals, as well as the departures, of each traffic flow associated to the users, hence somehow achieving the same result.

4.1.3. Link Adaptation

The purpose of the link adaptation is to identify the Modulation and Coding Scheme (MCS) that is more appropriate for the channel quality perceived by each user. In fact, a modulation level that is too high could theoretically transmit more data, but it would also result in many more errors at the physical layer, thus nullifying the advantage. Instead, a modulation level that is too low would result in lower speed without any significant gain. To this aim, it is of the utmost importance to find the optimal MCS. Basically, the users compute the Channel Quality Indicators (CQIs), i.e., quantized Signal to Interference plus Noise Ratio (SINR) values obtained through the estimation of the channel quality. Then, they feedback the CQIs to the base station (reporting procedure), which is in charge of mapping them to MCS indexes. An MCS index is used together with the number of resource blocks (as well as the number of spatial layers) to find the net amount of payload bits that can be transmitted to the user, as seen at the MAC layer, namely Transport Block Size (TBS), following a standardized procedure [64]. The `AMCModule` class is in charge of conducting this entire procedure during the resource allocation.

4.2. Supporting Models of 5G-air-simulator

This section will provide an overview of the main models developed for supporting 5G related Technical Components, which will be discussed in later Sections. In particular, supporting models of *5G-air-simulator* include a calibrated Link-to-System (L2S) model, a MIMO module, and a system-level implementation of the HARQ procedure.

4.2.1. Calibrated Link-to-System Model

The L2S model has the main purpose of quantifying the effectiveness of radio transmission, taking into account many phenomena, such as propagation and interference [65]. In a system-level simulator, this task should be accomplished without requiring explicit modeling of all the involved details, which would result in excessive complexity and very long running times. Instead, link-to-system models provide a simplified description of the phenomena of interest, which is still sufficiently accurate for the purpose of simulating a large system. Figure 3 depicts the main blocks of the link-to-system model designed for the *5G-air-simulator*. The preliminary assumption in *5G-air-simulator*'s L2S

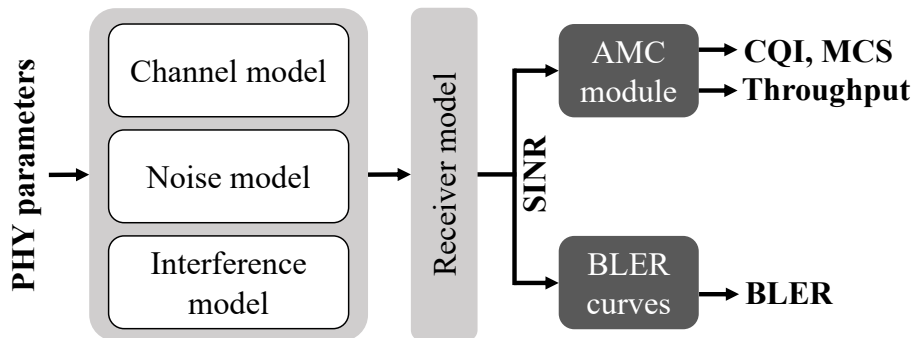


Figure 3: Components of the implemented link-to-system model.

model is that each transmitted signal is represented by its power spectral density value. Then, channel, noise, and interference models describe how this transmitted signal is seen at the receiver [66]:

- Channel models calculate the attenuation of the signals due to propagation, and they are composed of different parts: path loss, shadowing, penetration loss, and fast fading [67]. Fast fading models describe the small-scale parameters, such as delays, powers, and directions of arrival and departure on a very short time scale, about the size of a Transmission Time Interval (TTI). These frequency selective channel variations, which are mainly due to multipath, are modeled with pre-computed traces generated according to tabulated distribution functions and random parameters, as described in [68–70]. The stored traces include the effect of time, frequency, and antenna correlation when MIMO transmission is used, as well as

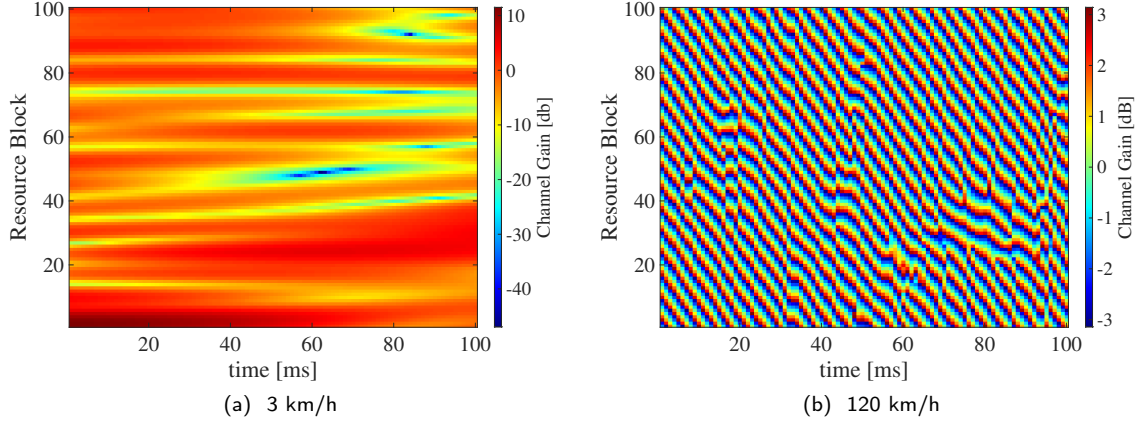


Figure 4: Fast fading realizations at different user speeds.

multiple interactions with the scattering media. A sample of the channel gains in the time-frequency domain for different user speeds is shown in Figure 4.

Shadowing is modeled as a log-normal variable, and penetration loss is usually set to a constant value for indoor users, but it may also be a random quantity too.

The path loss depends mainly on the distance, the frequency, and the environment [71]. The models included in *5G-air-simulator* are reported in Table 3 and Table 4, where the meaning of the most commonly used symbols is as follows: d is the distance between the base station and the user in km, d_{3D} is the 3D distance (including heights in the computation), f is the center frequency in GHz, H_{gnb} is the height of the base station, H_b is the average height of the buildings around it, and H_{ue} is the height of the mobile user.

It is worth mentioning that other minor phenomena usually affecting radio channels, e.g., blockage, are not modeled in order to maintain the complexity of the L2S model at an acceptable level.

- The noise power is calculated as simple thermal noise, with a spectral density of -174 dBm/Hz that is integrated over the bandwidth of one resource block.
- The interference power is modeled as the sum of the contribution from all the base stations (except for the serving base station), again using all the channel models as described above.

After the reception, the receiver has an SINR value for each resource block n , i.e. $\gamma(n)$. For more details, see Section 4.2.2, which thoroughly describes how the SINR is computed based on the selected transmission settings.

These SINRs need to be mapped to a single effective SINR value, reflecting the overall quality of the radio channel. Although different algorithms exist for this calculation, *5G-air-simulator* utilizes the Mutual Information Effective SINR Mapping (MIESM) method [76], which is known to provide good results with minimal tuning. Let \mathcal{N} , N , $I(\cdot)$, and β be the set of resource blocks assigned to the user, the cardinality of \mathcal{N} , the mutual information function, and a parameter that can be adjusted to match specific combination of modulation schemes, respectively. Then, the effective SINR, namely $\bar{\gamma}$, is computed as:

$$\bar{\gamma} = \beta I^{-1} \left(\frac{1}{N} \sum_{n \in \mathcal{N}} I \frac{\gamma(n)}{\beta} \right). \quad (1)$$

Note that $\bar{\gamma}$ is used for two different purposes. First, it is exploited to estimate the BLock Error Rate (BLER) for the received data block using the SINR-BLER curves in Figure 5, which determines the probability that it has been received and must be discarded. Second, it is sent to the base station to inform it of the perceived channel quality through CQI feedbacks, so that it can properly perform the link adaptation procedure (as explained in Section 4.1.3).

It is worth mentioning that although popular SDR platforms [77, 78] and link-level simulators may be used to deeply investigate topics limited to a reduced number of communication links, the obtained results can be leveraged to

Table 3
Baseline path loss models available in *5G-air-simulator*.

Name	Formula (dB)	Notes
Urban Macro-cell [72]	$80 + 40 \times (1 - 4 \times 0.001 \times (H_{gnb} - H_b)) \times \log_{10}(d \times 0.001) - 18 \times \log_{10}(H_{gnb} - H_b) + 21 \times \log_{10}(f)$	
Suburban Macro-cell [72]	$128.1 + (37.6 \times \log_{10}(d \times 0.001))$	
Rural Macro-cell [72]	$69.55 + 26.16 \times \log_{10}(f) - 13.82 \times \log_{10}(H_{gnb}) + (44.9 - 6.55 \times \log_{10}(H_{gnb})) \times \log_{10}(d \times 0.001) - 4.78 \times \log_{10}(f)^2 + 18.33 \times \log_{10}(f) - 40.94$	
Urban Micro-cell [72]	$24 + (45 \times \log_{10}(d))$	
Urban Femto-cell [73]	$\max(45, 127 + (30 \times \log_{10}(d \times 0.001))) + 18.3 \times n^{((n+2)/(n+1)-0.46)}$	
Winner downlink [74]	$A \times \log_{10}(d) + B + C \times \log_{10}(2.0/5.0) + 10.0 \times nbWalls[1] + 20.0 \times nbWalls[0]$	$LOS : A = 18.7, B = 46.8, C = 20.0$ $NLOS : A = 20.0, B = 46.4, C = 20.0$ $nbWalls[0]$ is the number of external walls, $nbWalls[1]$ is the number of internal walls
Basic downlink	$37 + (30 \times \log_{10}(d))$	

build additional supporting models to be integrated into *5G-air-simulator*, e.g., new modulation and coding schemes, BLER/BER curves.

An important property that simulation tools can have is the calibration of the channel models. Having calibrated channel models means that the outcomes of specific simulations have been compared to those of other similar products considering the same scenario, and channel models and settings have been adjusted until the results are similar. The calibration is important to ensure that there are no major errors in the implementation and that results from different solutions can be compared without incurring into unwanted misalignments. The simulation assumptions and the reference data are available in [79] and [80], while the most relevant parameters are summarized in Table 5. 3D channel models [69, 70] are embraced in the calibration process, taking into account time, space, and frequency correlation. As an example, Figure 6 and Figure 7 show the calibration results for the path gain and the SINR in the reference urban scenario, confirming that *5G-air-simulator* is well-calibrated. Similar results can be obtained for the other scenarios, like suburban or rural.

4.2.2. MIMO

In general, a MIMO system can be modeled according to Figure 8. During the precoding step, the user data has to be mapped to the available antennas in an appropriate way, since the radio channel is multi-dimensional due to multiple transmit and receive antennas. The goal of precoding is to make good use of the spatial degrees of freedom. In particular, the latter is better achieved when some information about the channel is available at the transmitter, usually thanks to the Channel State Information (CSI) reporting procedure. Such information can be acquired via a channel estimation procedure, however, that is not done in all cases. Contrarily, channel information is always required at the receiver. It is acquired at the same time as the user data via training signals, and it is used in the post-coding phase to reconstruct the original data. Different MIMO schemes differ in how the precoding, post-coding, and channel estimation functions are designed. In LTE and LTE-A, the configuration of specific MIMO features is done with the so-called Transmission Modes (TMs): communication with any given user can be configured with one of the available TMs, which dictates whether MIMO is used and what specific technique is employed. The presented version of *5G-air-simulator* supports the following TMs in downlink, derived from LTE specifications [81]

- TM1, single antenna transmission. The base station does not use any MIMO capability, however, if the mobile node is equipped with multiple antennas, it may still adopt Maximum Ratio Combining for improving the SINR. Let, $P_{tx}^{(j)}$ be the total transmit power from j-th base station (per cell), $P_{loss}^{(j)}$ the distance-dependent path loss, including shadowing and antenna gain/loss, $H^{(j)}(n)$ the channel gain from the j-th base station on the n-th sub-channel, N_r the number of receive antennas, $H_r^{(j)}(n)$ is the channel gain from the j-th base station to the r-th receive antenna on the n-th sub-channel, σ^2 the AWGN noise variance, and N_I the number of interferers. In the

Table 4

 Extended path loss models available in *5G-air-simulator*.

Name	Formula (dB)	Notes
Urban Macro-cell IMT (LOS, $d < d_{bp1}$) [68]	$22.0 \times \log_{10}(d) + 28 + 20 \times \log_{10}(f \times 0.001)$	$d_{bp1} = 4 \times (H_{gnb} - 1) \times (H_{ue} - 1) \times (f/300)$
Urban Macro-cell IMT (LOS, $d > d_{bp1}$) [68]	$40 \times \log_{10}(d) + 7.8 - 18 \times \log_{10}(H_{gnb} - 1) - 18 \times \log_{10}(H_{ue} - 1) + 2 \times \log_{10}(f \times 0.001)$	
Urban Macro-cell IMT (NLOS) [68]	$161.04 - 7.1 \times \log_{10}(20) + 7.5 \times \log_{10}(H_b) - (24.37 - 3.7 \times (H_b/H_{gnb})^2) \times \log_{10}(H_{gnb}) + (43.42 - 3.1 \times \log_{10}(H_{gnb})) \times (\log_{10}(d) - 3) + 20 \times \log_{10}(f \times 0.001) - (3.2 \times \log_{10}(11.75 \times H_{ue}))^2 - 4.97$	
Urban Macro-cell IMT-3D (LOS, $d < d_{bp1}$) [75]	$22.0 \times \log_{10}(d_{3D}) + 28 + 20 \times \log_{10}(f \times 0.001)$	$d_{bp1} = 4 \times (H_{gnb} - 1) \times (H_{ue} - 1) \times (f/300)$
Urban Macro-cell IMT-3D (LOS, $d > d_{bp1}$) [75]	$40 \times \log_{10}(d_{3D}) + 28 + 20 \times \log_{10}(f \times 0.001) - 9 \times \log_{10}(d_{bp1}^2 + (H_{gnb} - H_{ue})^2)$	
Urban Macro-cell IMT-3D (NLOS) [75]	$161.04 - 7.1 \times \log_{10}(20) + 7.5 \times \log_{10}(H_b) - (24.37 - 3.7 \times (H_b/H_{gnb})^2) \times \log_{10}(H_{gnb}) + (43.42 - 3.1 \times \log_{10}(H_{gnb})) \times (\log_{10}(d_{3D}) - 3) + 20 \times \log_{10}(f \times 0.001) - (3.2 \times \log_{10}(17.625)^2 - 4.97) - 0.6 \times (H_{ue} - 1.5)$	
Rural Macro-cell IMT (LOS, $d < d_{bp}$) [68]	$20 \times \log_{10}(40 \times \pi \times d \times (f \times 0.001/3)) + \min(0.03 \times H_b^{1.72}, 10.00) \times \log_{10}(d) - \min(0.044 \times H_b^{1.72}, 14.77) + 0.002 \times \log_{10}(H_b) \times d$	$d_{bp} = 2 \times \pi \times H_{gnb} \times 1.5 \times (f/300)$
Rural Macro-cell IMT (LOS, $d > d_{bp}$) [68]	$20 \times \log_{10}(40 \times \pi \times d_{bp} \times (f \times 0.001/3)) + \min(0.03 \times H_b^{1.72}, 10.00) \times \log_{10}(d_{bp}) - \min(0.044 \times H_b^{1.72}, 14.77) + 0.002 \times \log_{10}(H_b) \times d_{bp} + (40 \times \log_{10}(d/d_{bp}))$	
Rural Macro-cell IMT (NLOS) [68]	$161.04 - 7.1 \times \log_{10}(20) + 7.5 \times \log_{10}(H_b) - (24.37 - 3.7 \times (H_b/H_{gnb})^2) \times \log_{10}(H_{gnb}) + (43.42 - 3.1 \times \log_{10}(H_{gnb})) \times (\log_{10}(d) - 3) + 20 \times \log_{10}(f \times 0.001) - (3.2 \times \log_{10}(11.75 \times 1.5))^2 - 4.97$	

general case, the SINR of the n-th sub-channel is computed as:

$$\gamma(n) = \frac{P_{tx} P_{loss} |H(n)|^2}{\sigma^2 + \sum_{j=1}^{N_I} P_{tx}^{(j)} P_{loss}^{(j)} |H^{(j)}(n)|^2}, \quad (2)$$

while in case of Maximum Ratio Combining:

$$\gamma(n) = \frac{P_{tx} P_{loss} \left(\sum_{r=0}^{N_R-1} |H_r(n)|^2 \right)^2}{\left(\sum_{r=0}^{N_R-1} |H_r(n)|^2 \right) \sigma^2 + \sum_{j=1}^{N_I} P_{tx}^{(j)} P_{loss}^{(j)} \left| \sum_{r=0}^{N_R-1} H_r(n) * H_r^{(j)}(n) \right|^2}. \quad (3)$$

- TM2, transmit diversity. Space-frequency coding is employed over 2 or 4 transmitting antennas, providing diversity and coding gain. The receiver may use one or multiple antennas. Given that $H_{t,r}^{(j)}(n)$ is the channel

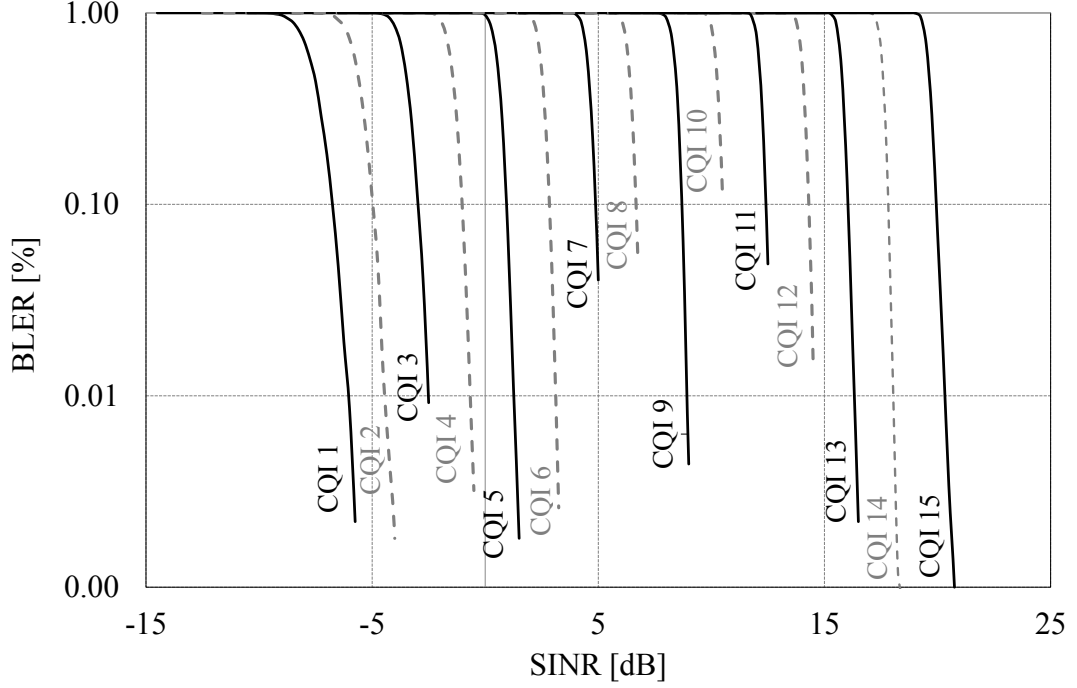


Figure 5: BLER curves for the link-to-system model obtained by MATLAB link-level Toolbox.

gain from the t -th transmit antenna of the j -th base station, to the r -th receive antenna, on the n -th sub-channel, the SINR is computed as:

$$\gamma(n) = \frac{P_S}{P_N + P_{I'} + P_{I''}}, \quad (4)$$

where:

$$\begin{aligned} - P_S &= P_{tx} P_{loss} \sigma^2 \left(\sum_{t=0}^1 \sum_{r=0}^{N_R-1} |H_{t,r}(n)|^2 \right)^2 \\ - P_N &= \left(\sum_{t=0}^1 \sum_{r=0}^{N_R-1} |H_{t,r}(n)|^2 \right) \sigma^2 \\ - P_{I'} &= \sum_{j \notin STBCset} P_{tx}^{(j)} P_{loss}^{(j)} \sigma_j^2 \left(\sum_{t=0}^{N_T^{(j)}-1} \left| \sum_{r=0}^{N_R-1} H_{0,r}(n)^* H_{t,r}^{(j)}(n) \right|^2 + \sum_{t=0}^{N_T^{(j)}-1} \sum_{r=0}^{N_R-1} H_{1,r}(n) H_{t,r}^{(j)}(n)^* \right) \\ - P_{I''} &= \sum_{j \in STBCset} P_{tx}^{(j)} P_{loss}^{(j)} \sigma_j^2 () \end{aligned}$$

- TM3, open-loop spatial multiplexing. This mode requires multiple antennas at both the transmitter and receiver, which are used to transmit multiple spatially multiplexed streams of data. The transmitter does not have fine-grained information about the MIMO channel, but only a Rank Indicator (RI). Hence, it uses a pre-defined and repeating sequence of precoding matrices, which is conceptually similar to periodically focusing the signal in different spatial directions. Receivers will get a good signal for some of the precoding matrices, and exploit the channel coding to recover the entire transmitted block from alternating good and bad observations.

Table 5

Calibration parameters for urban scenario

Parameter	Value
Carrier Frequency	2.0 GHz
Inter Site Distance	500 m
Bandwidth	10 MHz
Penetration Loss	0 dB
Speed	30 km/h
Cellular layout	Hexagonal grid, 19 cell sites, 3 sectors per site
Number of users per cell	10
Antenna pattern (horizontal)	$\phi_{3dB} = 70^\circ, A_m = 20dB$
Antenna pattern (vertical)	$\theta_{3dB} = 15^\circ, A_m = 20dB$
Noise Figure	5 dB
Base station max antenna gain	17 dBi
Base Station Antenna height	25 m
Total BS transmit power	46 dBm
Minimum distance between User Terminal and Serving Cell	25 m
Duplex method	FDD
Downlink transmission scheme	1x2 SIMO
Downlink Scheduler	Round robin with full bandwidth allocation
CQI reporting	Wideband CQI, 5 ms periodicity, 6 ms delay total. CQI measurement error: None.
Downlink HARQ	Maximum four transmissions
Downlink HARQ	Maximum four transmissions
Downlink receiver type	MRC
Antenna configuration	Vertically polarized antennas 0.5 wavelength separation at UE, 10 wavelength separation at base station
Channel estimation	Ideal, both demodulation and sounding
BS antenna downtilt	12 deg
BS feeder loss	2 dB

- TM4, closed-loop spatial multiplexing. In this case, the mobile station provides the base station some information about the MIMO channel, in the form of Precoding Matrix Indicators (PMIs) and RIs. The PMI instructs the base station to use a specific precoding matrix from a shared codebook for the precoding, thus ensuring that the MIMO transmission is adapted to the instantaneous channel characteristics. This allows a higher throughput compared to open-loop MIMO but has the downside that much more information has to be transmitted on the reverse link, from the user to the base station. The maximum antenna configuration is 4x4, with a peak throughput up to 4 times greater than TM1.
- TM9, 8-layer MIMO. This mode was introduced in Release-10 and allows up to 8x8 MIMO with twice the throughput of TM4. PMI is still transmitted using an extended codebook, using twice as many bits as the TM3/TM4 codebook, but in this case, the base station is not necessarily constrained to use one of the codebook's matrices for precoding.

For TM3, TM4, and TM9, the SINR is computed as:

$$\gamma_k(n) = \frac{\text{diag} [\sigma^2 D(n) D^*(n)]_{kk}}{\text{diag} \left[\sigma^2 W^*(n) W(n) + \sigma^2 I_{self} I_{self}^* + \sum_{j=1}^{N_I} P_{tx}^{(j)} P_{loss}^{(j)} \sigma_j^2 W^*(n) H^{(j)}(n) H^{(j)*}(n) W(n) \right]_{kk}}, \quad (5)$$

where:

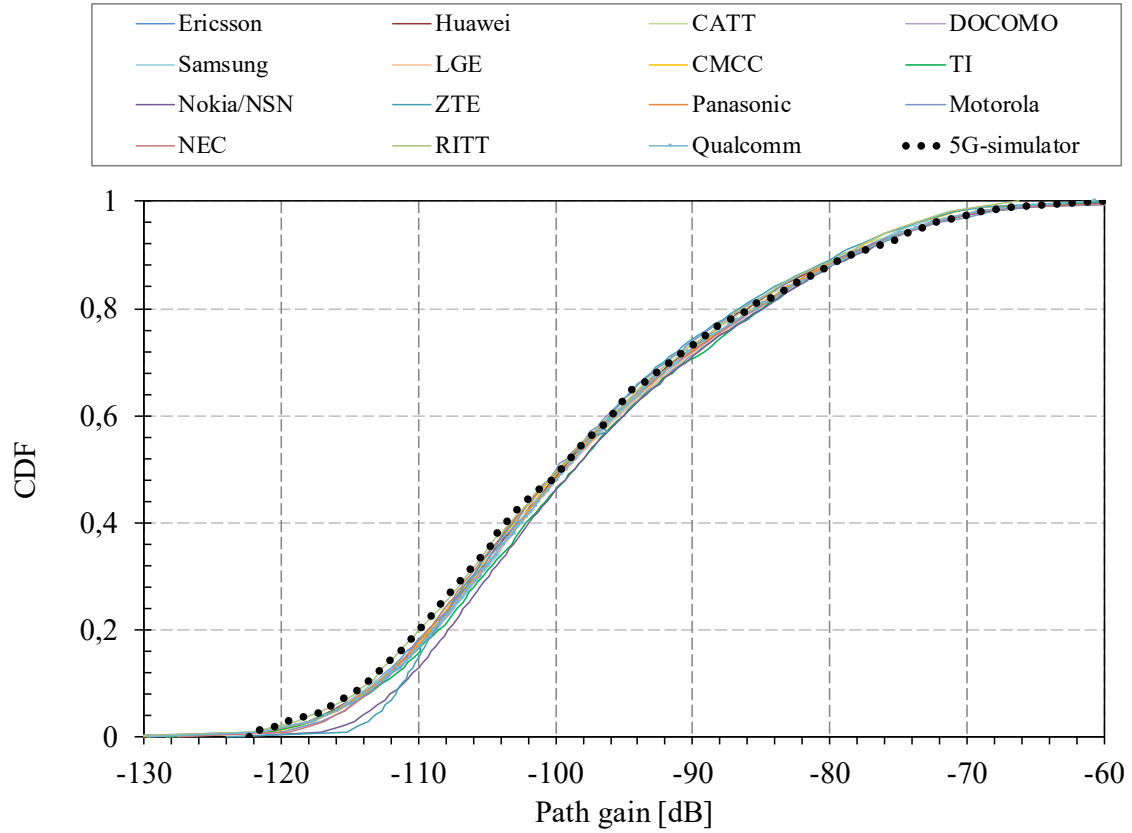


Figure 6: Calibration of path gain (urban scenario).

- $D(n) = \text{diag} \left[W^*(n) \sqrt{P_{tx}} P_{loss} H(n) \right]$
- $I_{\text{self}}(n) = W^*(n) \sqrt{P_{tx}} P_{loss} H(n) - D(n)$
- $W(n) = \left(\sigma^2 P_{tx} P_{loss} H(n) H(n) + \tilde{\sigma}^2 \right)^{-1} \sigma^2 \sqrt{P_{tx} P_{loss}} H(n)$
- $\tilde{\sigma}^2 = \sigma^2 I + \sum_{j=1}^{N_h} \sigma_j^2 P_{tx}^{(j)} P_{loss}^{(j)} H^{(j)}(n) H^{(j)*}(n)$
- $H^{(j)}(n)$ is the channel gain matrix from the j -th base station.

Note that, without loss of generality, all the symbols without the index j are related to the target user/base station.

4.2.3. HARQ Procedure

HARQ is a retransmission method that works at the boundary between physical and MAC layers. It is a base feature of high-speed mobile networks, so it has been implemented in *5G-air-simulator* as well [82]. There are few variants of it, but the simulator currently supports chase combining (also called HARQ type I), which works in the following way:

- the transmitter sends a data block, encoded with a Forward Error Correction (FEC) code which allows error detection and correction to a certain extent.

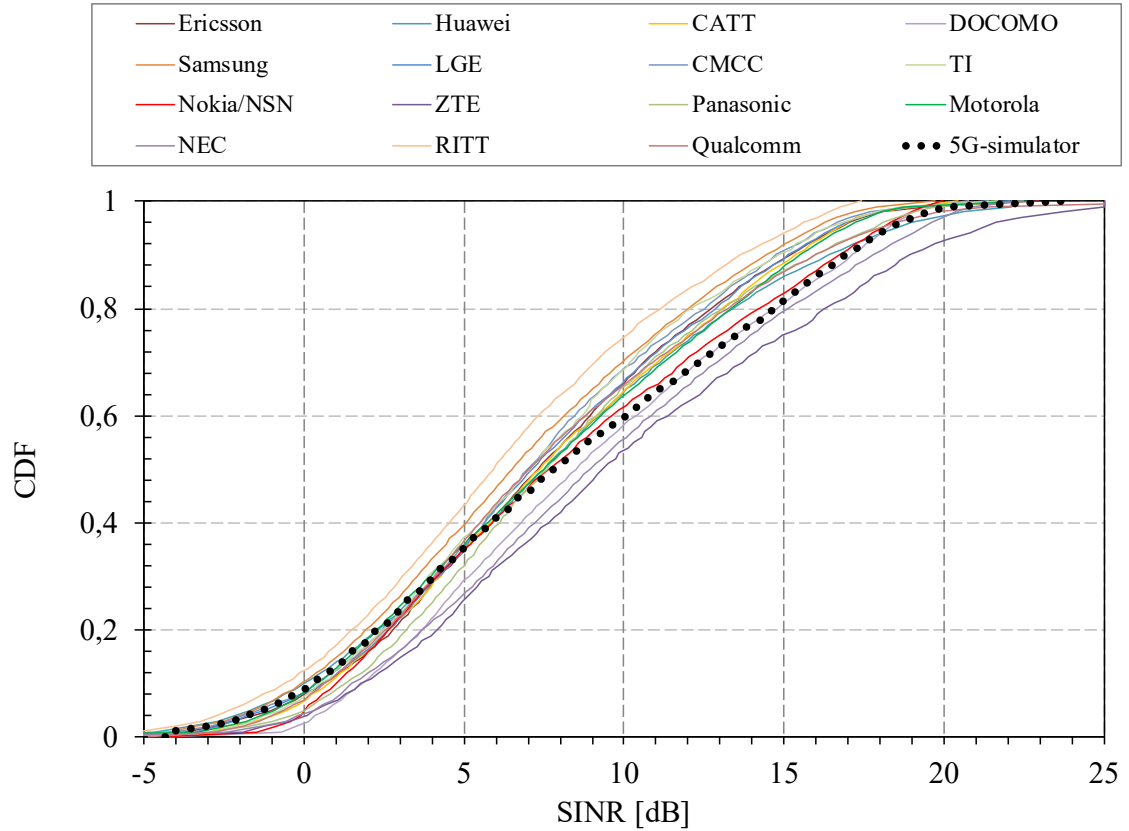


Figure 7: Calibration of SINR (urban scenario).

- The receiver checks the received blocks for errors. If there are no errors, or the errors can be recovered, then a positive acknowledgment (ACK) is sent back and transmission is completed successfully. If there are non-recoverable errors, the received signal is held into a buffer and a negative acknowledgment (NACK) is sent.
- Upon receiving a NACK, the transmitter re-sends the same block again.
- The receiver gets a second copy of the message, which is combined via Maximum Ratio Combining (MRC) with the previous copy to increase the SINR. If the combined copy is now decodable an ACK is reported otherwise a NACK is returned.
- The transmission is repeated until the block can be decoded or the maximum number of attempts is reached.

Differently from plain Automatic Repeat reQuest (ARQ), which considers each retransmission separately, HARQ takes advantage of the combination of multiple copies of the signal. In the case of chase combining, the result is similar to the use of an additional repetition coding. Since the back-and-forth of HARQ may require some time, the receiver could remain stuck on a given block and unable to receive additional data. To avoid this, multiple HARQ sessions can be simultaneously active. These are called HARQ processes and up to 8 can be instantiated for each receiver, as the latency for single retransmission is typically 8 sub-frames. However, since HARQ is modeled from a system-level point of view, the number of processes, as well as their timers, may be set to custom values in order to speed up the entire procedure. In other words, the delay introduced by the HARQ procedure may be manually adjusted by defining a different ACK waiting time interval.

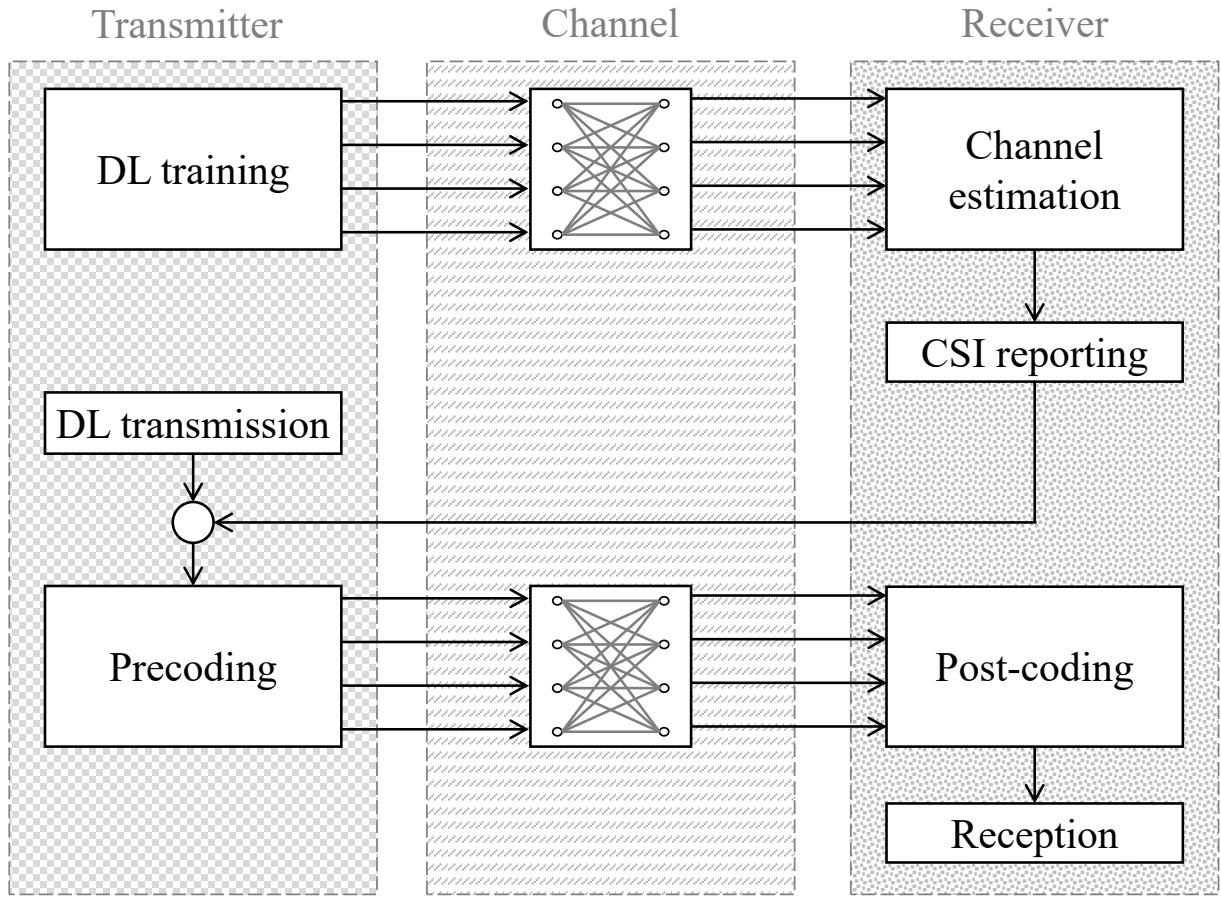


Figure 8: Block diagram of a MIMO system.

4.3. Simulation Tracing

5G-air-simulator provides a text trace during the execution of the simulation. Figure 9 shows an example of the text trace. The first field of each line reports the event that triggered the tracing. Specifically, rows starting with TX, RX, and DROP are associated with packets that have been sent, received, and dropped, respectively. In addition, a line starting with PHY_RX indicates a reception event at the physical layer, while RANDOM_ACCESS provides information about the random access procedure. For lines related to packets, the second field describes the application type. SRC and DST identify the nodes that send and receive the packet, respectively, while ID identifies the packet uniquely, and B the bearer used to map the packet. The value after D during reception events represents the delay of the received packet in seconds. In general, T reports the time instant in which an event occurred, in seconds (TIME, instead, is in ms).

The main performance indicators can be retrieved by redirecting the console output of each simulation run to a different file and then extracting the relevant data. The main KPIs may be computed as follows.

- **Average User Throughput:** it is necessary to consider all the lines starting with the keyword PHY_RX and sum all the values appearing at the 17th position (indicating the transport block size in bits), but only when the value at the 19th position is 0 (indicating no reception errors). The resulting values should then be divided by the number of active users in the simulation.
- **Average Packet Loss Ratio (PLR):** it is calculated as the ratio of lost packets over total transmitted packets at the application layer. In this case, the transmitted packets correspond to the number of lines starting with TX, while the received packets are identified by the number of lines starting with RX.

```

RX CBR ID 119 B 0 SIZE 20 SRC 3 DST 0 D 0.003 0
      Packet Size [byte]
RANDOM_ACCESS COLLISION UE 12 PREAMBLE 7 TIME 48

DROP VIDEO ID 681 B 29
      Application
PHY_RX SRC 2 DST 7 X 240 Y -130 SINR 3.9366 RB 13 MCS 13 SIZE 1131 ERR 1 T 0.052
PHY_RX SRC 2 DST 3 X 199 Y 199 SINR 10.3639 RB 73 MCS 21 SIZE 113122 ERR 0 T 0.052
TX INF_BUF ID 120 B 1 SIZE 1490 SRC 2 DST 3 T 0.052 0
PHY_RX SRC 2 DST 3 X 199 Y 199 SINR 10.1639 RB 100 MCS 15 SIZE 114672 ERR 0 T 0.053
      Destination Node ID      Number of RB      TBS [bit]

```

Figure 9: Example of the text trace of a simulation.

- **Average Random Access Collision Rate:** Similarly to the PLR, it is defined as the ratio between preamble collisions and successful completions. It is necessary to consider all the lines starting with the keyword `RANDOM_ACCESS COLLISION` to identify the collisions. On the other hand, the lines starting with `RANDOM_ACCESS RECEIVE_MSG4` indicate the procedure ending.
- **Cell Goodput:** consider the lines starting with the keyword `RX` and sum all the values appearing at the 8th position, indicating the application data size in byte. Then, the sum must be multiplied by 8 and divided by the simulation duration in order to obtain the goodput in bps.
- **Average Packet Delay:** The 14th position of all the lines starting with `RX` are already expressed in seconds. It is sufficient to collect all these values and compute their average.
- **Cell-Edge Throughput:** it is typically calculated as the 5%-ile of the throughput values achieved by the users. Similarly to the average user throughput, this can be extracted from the lines starting with `PHY_RX`, by summing the values on the 17th field only when the 19th field is 0. However, in this case, this should be done separately for each receiving user, i.e., for every different value of the 5th field. Finally, the Empirical Cumulative Distribution Function (ECDF) of the values obtained for each user should be computed and the value corresponding to the 5% is taken as the cell-edge throughput.

Since the text trace contains much information, on the basis of the proposed approaches, further investigations are still possible in order to derive finer-grained or more detailed results.

At the time of this writing, *5G-air-simulator* already comes with a number of GNU AWK [83] tools for processing the text trace of a simulation. For instance, `make_goodput` and `make_plr` compute the related KPIs, `make_cdf` computes the Empirical CDF of packet delays, the overall spectral efficiency for a given assigned bandwidth is given by `make_cell_spectral_efficiency` and `make_fairness_index` returns the Jain's fairness index, while `make_avg` is a general script to compute the average of a text input.

4.4. User-defined Scenarios

5G-air-simulator already implements a wide set of simulation scenarios, willing to test and investigate SISO, MIMO, and Massive MIMO deployments, multicast and broadcast transmissions, high-speed use cases, and massive IoT and NB-IoT deployments. According to the guidelines provided by standardization documents and scientific literature, each simulation scenario implements specific network deployment, physical, channel, application, and mobility models. The test can be executed through a command-line instruction, that contains the name of the software executable, the name of the reference scenario to be investigated, and a list of parameters to generally control simulation details. For instance, they include the number of cells, the number of users, the number and type of applications, the

user speed, physical and channel details, the scheduling algorithm, and some other technical details properly related to the technical component of interest.

Besides, one of the main advantages of *5G-air-simulator* is that users can define additional customized simulation scenarios. The first simple way to customize the simulations is by considering a specific parameter set for the list of input arguments for each selected use case, to evaluate its performance. It is important to emphasize that this approach ensures an effective usage of the tool for users willing to evaluate the performance of customized use cases without requiring the editing of C++ sources.

As a second way to customize their simulations, users can extend the reference C++ library implementing a given use case and modify available settings. Possible modifications may refer to network deployment (e.g., position of base stations), physical settings (e.g., transmission mode, transmission power, number of transmitting and receiving antennas, and noise figure, plus, for base stations only, antenna bearing, e-tilt, antenna gain, horizontal and vertical beamwidth at 3 dB, feeder loss, and maximum horizontal and vertical attenuation), channel model (e.g., rural vs urban, path loss model, fading parameters), application level (e.g., number and type of applications per user, time instant in which every single application starts and stops), and mobility models (e.g., static position, random direction, linear movement). However, differently from the previous approach, users have to modify the source code, by integrating available models within their simulation scenario. This activity requires a minimum level of knowledge of C++. In particular, a custom scenario can be created as a static function in a proper header file, which should also be included in the main program. In general, a basic scenario includes an instance of `Simulator`, `NetworkManager`, `FlowsManager`, and `FrameManager` components, cells, gNBs, and UE objects, several applications, and the `Simulator::Run()` function.

The third methodology offering the possibility to define custom simulation scenarios is rooted in the flexibility and extensibility of *5G-air-simulator*. It can be adopted to effectively pursue new research questions arising from new applications/services and features, allowing researchers and practitioners to test, extend, and evaluate the advanced solutions for 5G. For instance, new technical components may be integrated to explore emerging research topics. Also, adding new mobility and application models is as simple as writing new classes derived from the baseline code. Clearly, this approach also requires a more complex intervention of tool's users, due to the need for developing new functionalities starting from baseline C++ classes already available into the simulator.

5. Massive MIMO

Massive MIMO is an important transmission technique in cutting-edge communication systems. By using numerous antennas it is possible to increase throughput, spectral efficiency, and coverage, depending on channel conditions. Moreover, the scientific literature demonstrated that Massive MIMO allows serving many users simultaneously, with a mutual interference that approaches zero, while achieving a very large sum spectral efficiency [84]. As a consequence, it is not surprising that it emerged as a key technical component for the NR. The scientific literature proposes various methodologies for implementing Massive MIMO in mobile networks. The one taken into account for the developed *5G-air-simulator* is based on the Joint Spatial Division and Multiplexing (JSDM) technique [85].

5.1. Theoretical Description of the Technical Component

Massive MIMO has been natively conceived to work in TDD operation mode, since channel reciprocity limits the overhead due to the training procedure (i.e., the base station is able to learn the channel quality experienced by mobile terminals in the downlink by evaluating the signal received in the uplink)[20, 36, 84]. Nevertheless, several works investigated new approaches for implementing Massive MIMO in FDD operation mode [86–90]. All of them introduce some strategies to deliver the downlink CSI feedbacks to the base station without incurring in high overhead. Among the possible solutions available in the literature, JSDM is a very promising and well-known approach implemented in *5G-air-simulator*. In line with the previous considerations, JSDM involves a 2-stage precoding scheme aimed at reducing the training overhead of Massive MIMO in FDD mode. Its block diagram is shown in Figure 10. From the system-level point of view, JSDM allows to send independent signals in fixed spatial directions, spanning the entire area of the cell sector. The resulting transmission is also referred to as Grid of Beams. To reach this goal, the precoding matrix is obtained as a combination of two matrices, one for each precoding stage. More specifically, the first stage precoder is used to capture the long-term and second-order channel statistics which are wideband and stable for a relatively long duration. At the receiver side, the precoded training signals are exploited to acquire long-term CSI, whose reporting ensures a limited training overhead. Instead, the second stage precoder is used to capture the

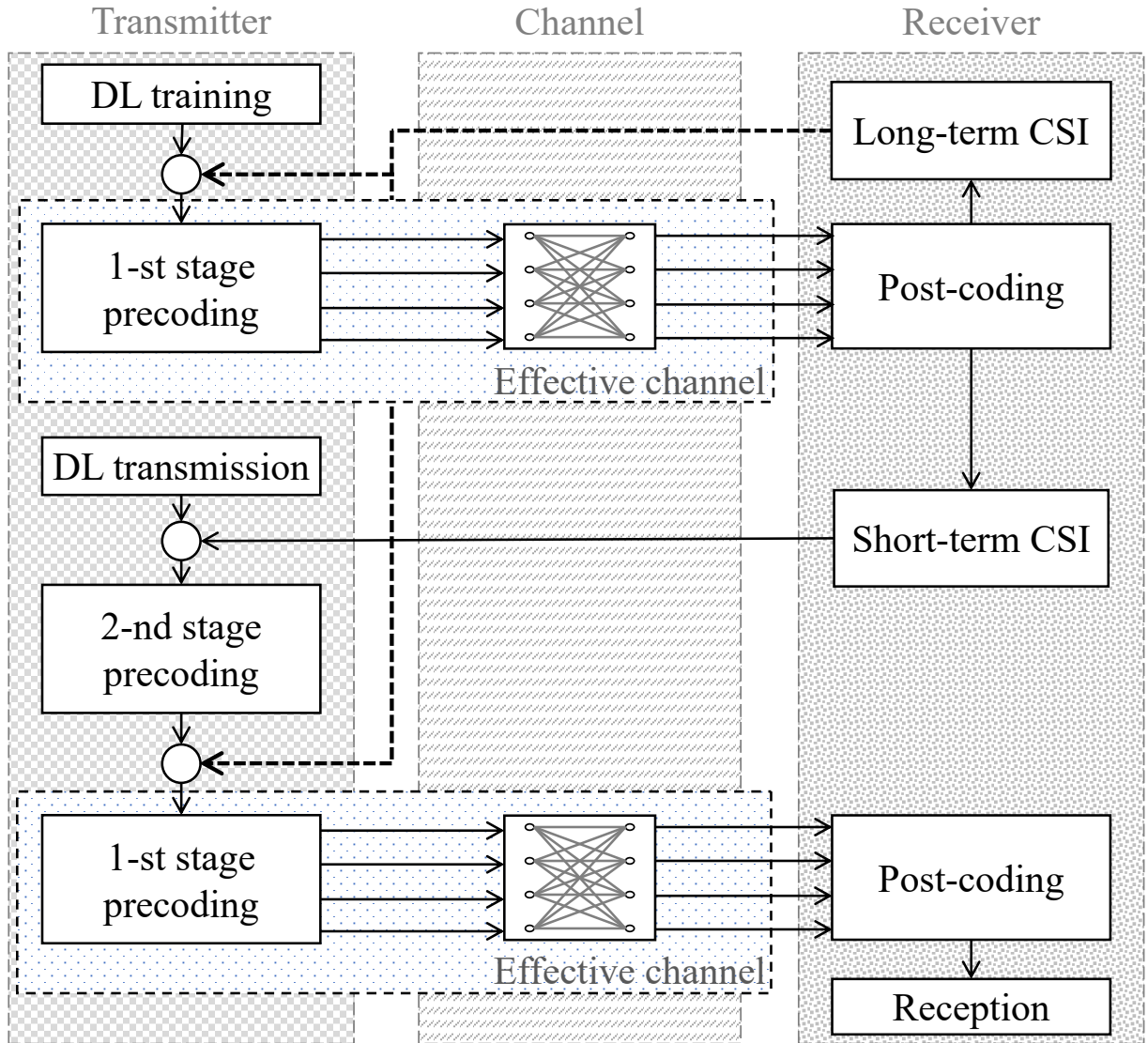


Figure 10: Block diagram of a JSDM Massive MIMO system.

short-term variation of the channel.

In this case, the resulting effective channel matrix has a reduced dimensionality, thanks to the utilization of the first-stage precoder. The second stage precoder is calculated by using the Regularized Zero-Forcing (RZF) scheme. Additionally, in order to improve JSDM performance levels, a multi-cell interference reduction technique can be implemented on top of the first-stage precoding. The approach developed in the *5G-air-simulator* uses the first-stage precoder also for beam coordination between base stations, hence achieving a flexible sub-sectorization of the covered geographical area. Specifically, three different configurations of beams are defined, which only cover a subset of the cell sector, instead of the entire sector as described above. Then, the configuration is frequently changed in a synchronized manner among nearby base stations in order to reduce the interference.

5.2. Main Implementation Details

The single antenna transmission technique, already available in the original version of the LTE-sim tool, requires to model the transmitted signal by means of a vector of elements describing the power density distributed across the

Table 6

Main functions related to MIMO and Massive MIMO features.

Key functionality	Class	Method	Parameters
Allocate the fast fading component of the channel model, considering the number of transmitting and receiving antennas	ChannelRealization	enableFastFading()	(none)
Update the fast fading realization	ChannelRealization	UpdateFastFading()	(none)
Get the propagation loss for each channel path	ChannelRealization	GetLoss()	(none)
Get the beamforming gain for a specific beam	ChannelRealization	GetBeamformingGain()	beam index
Get the beamforming gain for a specific beam and coordination pattern	ChannelRealization	GetBeamformingGain_cover()	beam index, beam coordination pattern index
Apply the propagation loss to a transmitted signal	PropagationLossModel	AddLossModel()	source node, destination node, signal
Allocate resource blocks to users, supporting multiple allocation with Massive MIMO	DownlinkPacketScheduler	RBsAllocation()	(none)
Receive a radio signal and calculate the SINR, including MIMO post-processing when required	UePhy	StartRx()	packet burst, signal
Create channel state feedbacks, including those for MIMO and Massive MIMO when required	UePhy	CreateCqiFeedbacks()	SINR vector

available/selected subchannels. To implement MIMO and Massive MIMO mechanisms, *5G-air-simulator* extends the baseline representation of the signal with a multidimensional approach. Rather than using a plain scalar number for each subchannel, the element of the transmitted or received signal becomes an array with a length equal to the number of transmitting or receiving antennas, respectively.

MIMO and Massive MIMO capabilities are mainly implemented in `ChannelRealization`, `PropagationLossModel`, `DownlinkPacketScheduler`, and `UePhy` classes, as summarized in Table 6. Transmission and reception procedures are handled by `DownlinkPacketScheduler` and `UePhy` classes, respectively. `DownlinkPacketScheduler` implements the transmitter process, including radio resource allocation, precoding operation, and simultaneous transmission to multiple users, which is a key advantage of Massive MIMO. On the other hand, `UePhy` is in charge of carrying out the reception of the radio signals and the SINR computation, as well as the calculation of CSI, when required. These values are forwarded to the base station, similarly to the CQI report, where they are used for the precoding operation. In order to perform the SINR computation, `ChannelRealization` and `PropagationLossModels` classes are used. In particular, the `ChannelRealization` class deals with fast fading and beamforming, according to the selected channel model. Instead, propagation loss is applied to each transmitted signal through the class `PropagationLossModels`. The SINR and CSI feedbacks are computed according to the procedures described in Section 4.2.1, which mimic the procedures already present in both LTE and NR standards.

5.3. Reference Test and Results

The performance of the Massive MIMO transmission scheme has been investigated by considering a practical implementation envisaged within the FANTASTIC-5G EU H2020 project. The reference scenario is based on the test-multi-cell-tri-sector deployment and each base station is equipped with a rectangular antenna array of 256 elements (16 horizontal elements \times 8 vertical \times 2 polarizations) [91]. At the application layer, the model is the `InfiniteBuffer` while the mobility model is `RandomWalk`. The first stage precoder is configured in order to achieve 16 horizontal beams with two alternating elevation angles. The packet scheduler supports 2 spatially multiplexed data streams per user. The scenario is called `f5g-uc1` because it models the use case 1 in the project's documentation and

Table 7

Adopted Values for the Parameters of the Scenario

Parameter	Value		
environment	"urban"	"suburban"	"rural"
isd	0.2 km	0.6 km	1 km
userDensity	2500 users/km ²	400 users/km ²	100 users/km ²
speed	3 km/h		
duration	10 s		
tm	9, 11		
nbTx	32 beams		
nbMu	8 users		
nbRx	2 antennas		
sched	round-robin		
seed	1-30		

the syntax used to perform the test is as follows:

```
./5G-air-simulator f5g-ucl env isd density speed time tm nTx nMu nRx sched (seed)
```

where

- env is the propagation environment used for channel models;
- isd is the Inter-Site Distance (ISD) in km;
- density is the user density measured in users/km²;
- speed is the speed of the mobile users in km/h;
- time is the duration in seconds of each simulation run;
- tm is the TM adopted for transmission, where values 1, 2, 3, 4, 9 have the same meaning as in the LTE specifications, and 11 represents Massive MIMO;
- nTx is the number of beams used at the base station for the first-stage precoding;
- nMu is the number of users that can be scheduled simultaneously for each resource block and TTI;
- nRx is the number of receiving antennas at the mobile terminals;
- sched is the scheduling algorithm;
- seed is an optional seed to initialize random quantities to different, but reproducible, values in each simulation run.

The performance of the developed Massive MIMO technique is evaluated in urban, suburban, and rural scenarios, with different parameter settings, as reported in Table 7. The main performance indicator that was considered is the user throughput. The results reported in Figure 11 demonstrate that Massive MIMO, implemented with the JSMD technique, can provide huge throughput gains over state-of-the-art LTE capabilities, up to around 800% when the beam coordination technique is employed. It is important to note that the subtle differences among different scenarios are also caused by a different traffic density (i.e. Gbps/km²) characterizing the environments, as reported in Figure 12.

6. Extended Multicast and Broadcast Transmission

Since the radio channel is intrinsically a shared medium, multicast and broadcast communication can be attained at the physical layer with relatively low complexity and high efficiency. This mode of operation can be very useful in some specific circumstances, e.g. for video broadcasting of a live event, software upgrades and so on. Since LTE Release 9, the support of multicast and broadcast communications has been provided through the MBSFN architecture

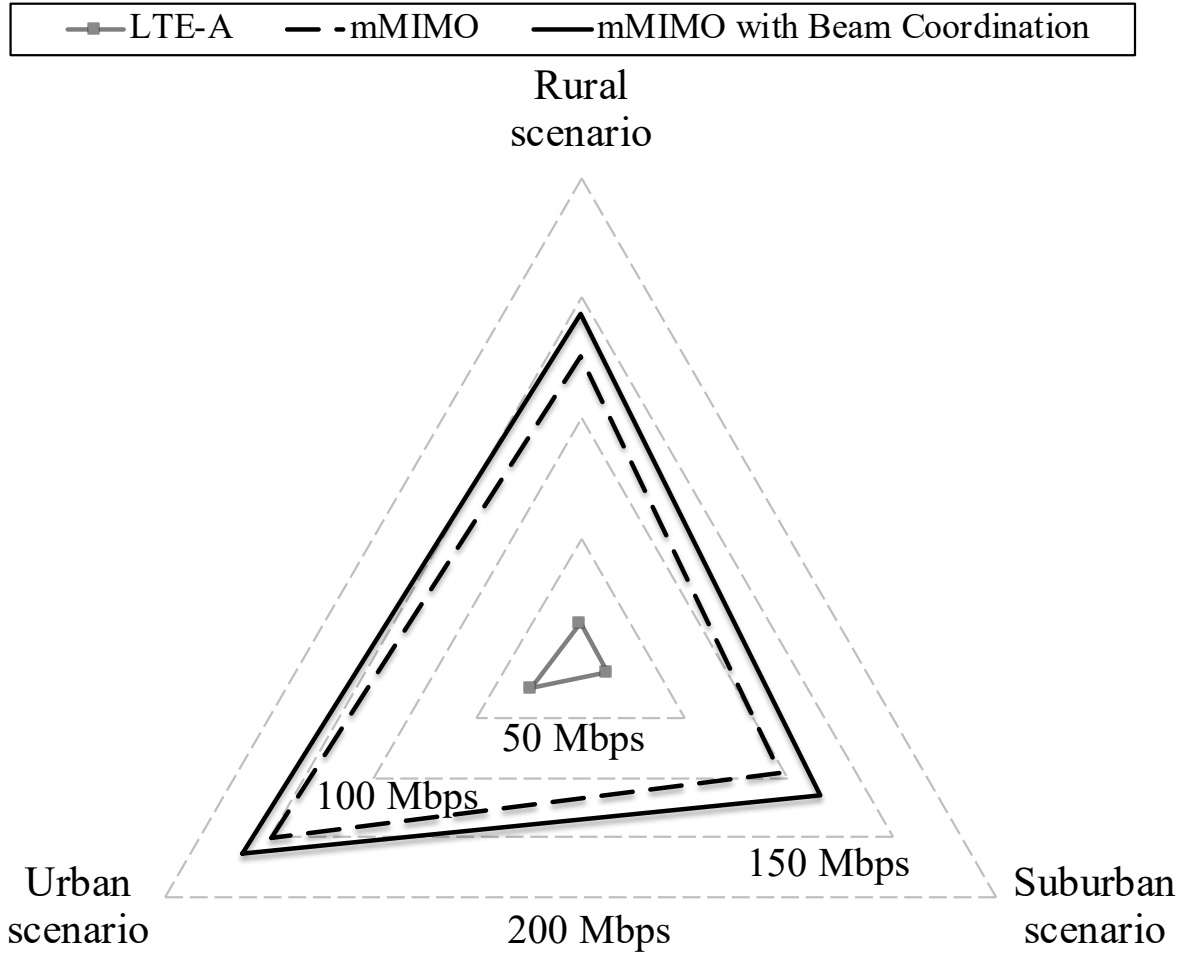


Figure 11: Throughput comparison between MIMO and Massive MIMO.

[19]. Today MBSFN still represents a technical component for 5G though some upgrades have been recently proposed in the scientific literature. Among them, adaptive MCS selection and HARQ retransmission [92] are those modeled within *5G-air-simulator*.

6.1. Theoretical Description of the Technical Component

With MBSFN, multiple base stations work in a coordinated manner to define a MBSFN area and the broadcast signal is transmitted on the entire bandwidth during pre-defined time slots. This mechanism brings to two main advantages. First, an extremely high bandwidth saving can be achieved, since many users can be served by using the same set of radio resources. Second, signals from multiple surrounding base stations can combine constructively if their delays are within the cyclic prefix duration, thanks to the properties of OFDM [93]. This improves communication performance and, most importantly, removes the main sources of interference.

A major drawback of the initial MBSFN architecture is that there is no reverse link between the base stations and the users. Thus, the base station has no knowledge of the users' channels, or whether packets are correctly received. For this reason, the MCS selection has to be very conservative and thus possibly inefficient.

5G intends to overcome this important limitation by introducing novel methodologies aiming at improving the overall communication process. In line with these premises, the EU H2020 FANTASTIC-5G project proposed to extend MBSFN beyond the original 3GPP standard with adaptive MCS selection and HARQ retransmissions func-

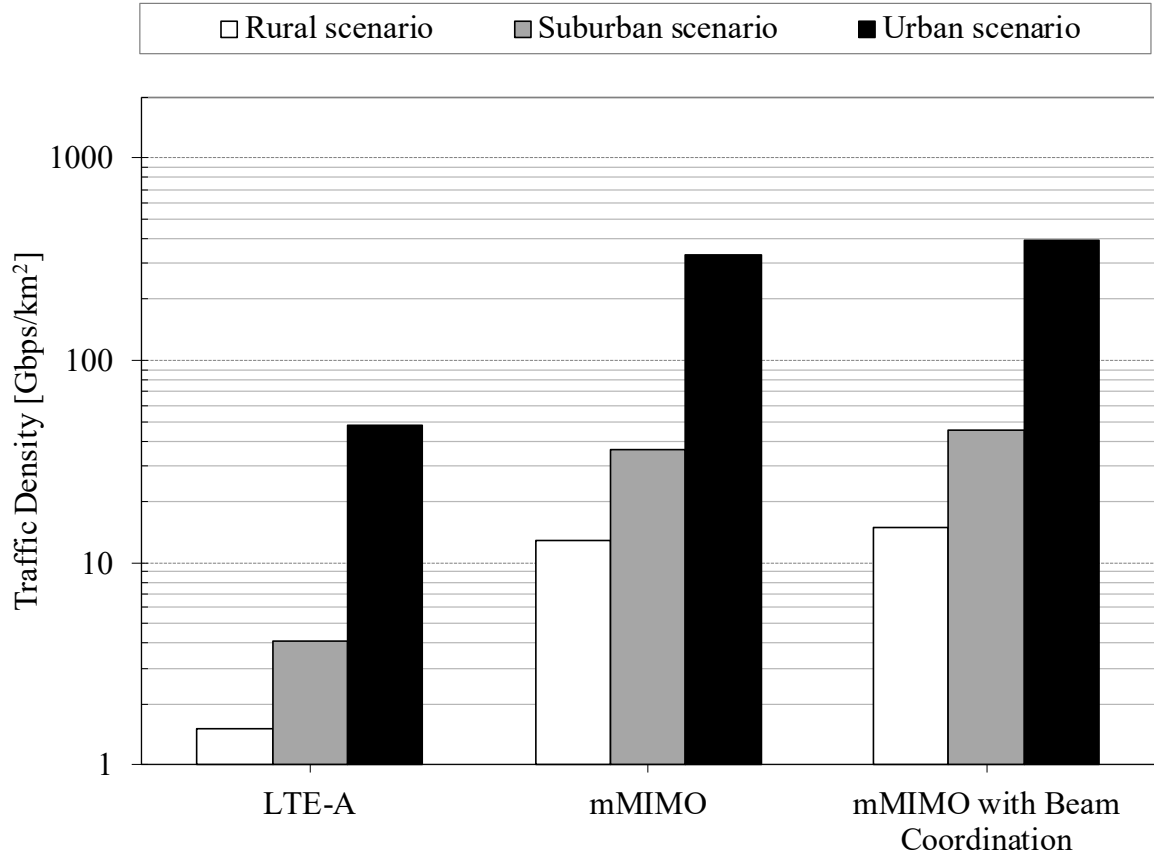


Figure 12: Traffic densities of the evaluated scenarios

tionalties [21]. Both rely on the introduction of a unicast uplink feedback channel for the MBSFN downlink channel. For the adaptive MCS selection, users send CQI feedbacks describing the quality of the broadcast channel, and the base stations perform the Link Adaptation procedure by selecting the most suitable MCS to be used for transmission so that all the users (or any desired fraction of them) can correctly receive the transmitted data. As for the HARQ retransmission, instead, users send an ordinary ack/nack feedback, i.e., as in the unicast case, and the packets that are lost are transmitted again. However, while the first transmission takes place on the MBSFN channel, subsequent re-transmissions are sent in unicast mode only to the interested users, so that more efficient techniques such as MIMO can be employed. Figure 13 shows the block diagram of the extended MBSFN architecture just discussed.

6.2. Main implementation details

Table 8 summarizes the main methods and classes involved in the multicast/broadcast operation. To implement the baseline MBSFN architecture in the *5G-air-simulator*, the classes `MulticastDestination` and `MulticastDestinationPhy` are derived from the classes `UserEquipment` and `UePhy`, respectively. `MulticastDestination` contains pointers to all the users receiving the broadcast signal. With this information, when an application flow is created with a `MulticastDestination` object as the receiver, a radio bearer sink for the corresponding radio bearer is created for each receiving user so that the transmitted packets are received by all the users belonging to the multicast group. At the same time, the downlink packet scheduler distributes resource blocks between unicast and multicast/broadcast communications according to a well-defined MBSFN frame structure [94]. Specifically, the `FrameManager` class is extended with the notion of MBSFN sub-frames and non-MBSFN sub-frames. Scheduling and transmission of MB-

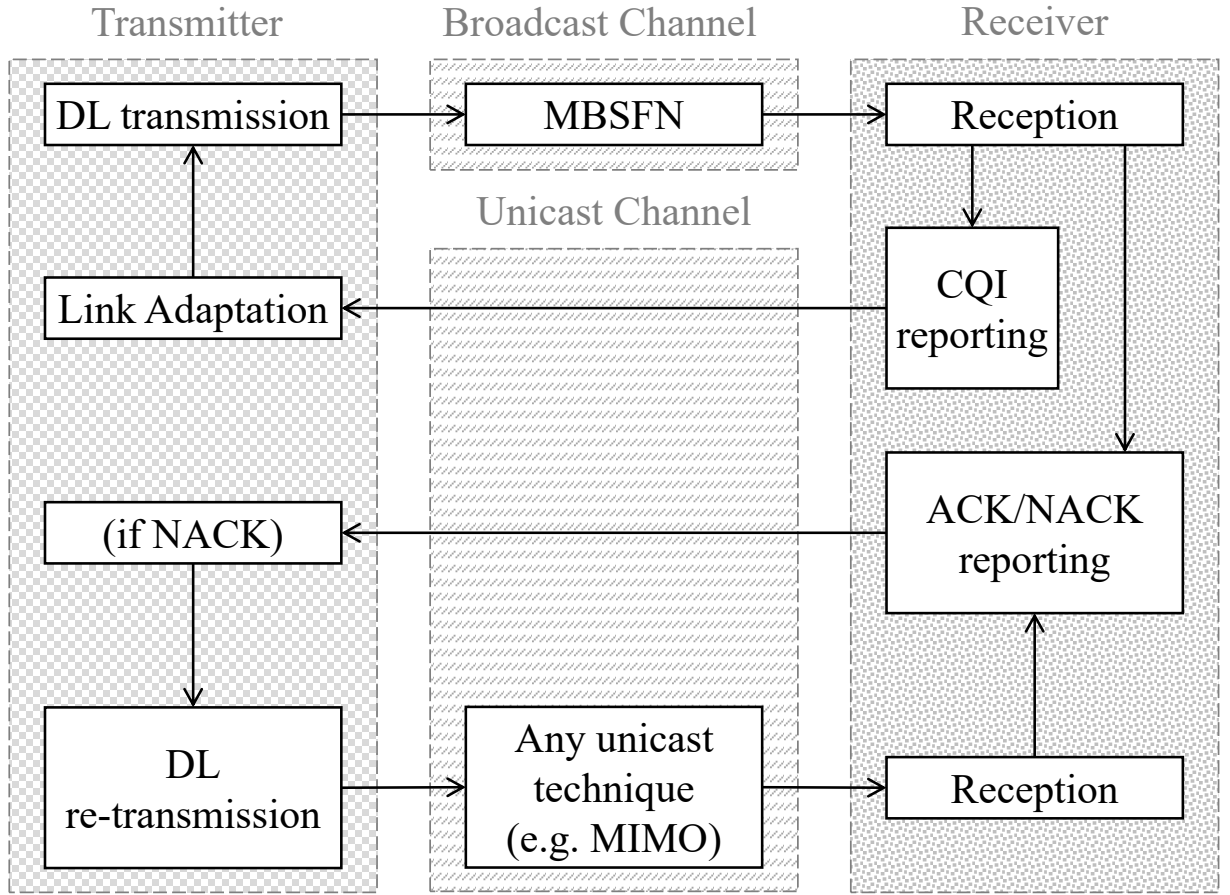


Figure 13: Block diagram of a MBSFN system with proposed extensions.

SFN and non-MBSFN applications flow only happens during the corresponding sub-frame type. According to the specifications, up to 6 sub-frames in a radio frame can be used for MBSFN operation, whose pattern is defined by using the `FrameManager::SetMbsfnPattern()` method and repeated cyclically for the entire simulation. Besides, the `Interference::ComputeInterference()` function already available in the original version of the LTE-Sim tool, has been extended in order to account for MBSFN operation: all the signal coming from the same MBSFN area are treated as useful signal rather than interference.

The adaptive MCS selection scheme is mainly implemented by the `MulticastDestinationPhy::CreateCqiFeedbacks()` method. In summary, it manages the collection of CQIs feedbacks of users receiving the multicast stream, and it helps the packet scheduler in the selection of the most suitable MCS index to be used for future multicast/broadcast communications (i.e., link adaptation). Particularly, the MCS selection may be done either by considering the absolute lowest CQI value of the multicast group or to ensure the correct reception of a pre-determined percentage of users.

As for the HARQ retransmissions, most of the features are modeled within the `DownlinkPacketScheduler` class. In `DownlinkPacketScheduler::RBsAllocation`, when a multicast flow is scheduled, multiple copies of the corresponding `PacketScheduler::FlowToSchedule` structure are created for each destination user, and they are added to the corresponding `HarqManager` object. Additionally, in `DownlinkPacketScheduler::DoStopSchedule()`, the packet burst of the original flow is copied in the duplicated flows. From then on, they act as any other unicast flow, including retransmissions.

Table 8

Main functions related to multicast/broadcast features.

Key functionality	Class	Method	Parameters
Create a multicast group on the given base station	MulticastDestination	MulticastDestination()	ID, cell, target BS
Add a base station to the multicast group	MulticastDestination	AddSource()	node
Remove a base station from the multicast group	MulticastDestination	DeleteSource()	node
Get the list of base station in the multicast group	MulticastDestination	GetSources()	(none)
Add a user equipment to the multicast group	MulticastDestination	AddDestination()	node
Remove a user equipment from the multicast group	MulticastDestination	DeleteDestination()	node
Get the list of user equipments in the multicast group	MulticastDestination	GetDestinations()	(none)
Create the physical layer interface for a multicast group	MulticastDestinationPhy	MulticastDestinationPhy()	(none)
Create the CQI feedbacks for a multicast group	MulticastDestinationPhy	CreateCqiFeedbacks()	(none)
Compute the inter-cell interference for a user equipment, assuming useful signal from base stations in the same multicast group	Interference	ComputeInterference()	user equipment, flag for MBSFN interference model
Set the number of sub-frames dedicated to MBSFN in each radio frame	FrameManager	SetMbsfnPattern()	number of MB-SFN sub-frames
Check whether MBSFN is enabled	FrameManager	MbsfnEnabled()	(none)
Check whether the current sub-frame is a MBSFN sub-frame	FrameManager	isMbsfnSubframe()	(none)
Allocate resource blocks in the downlink. During MBSFN sub-frames, all the resource blocks are allocated to all the users of the multicast group	DownlinkPacketScheduler	RBsAllocation()	(none)

6.3. Reference Test and Results

An example network configuration taken into account to evaluate the performance of the aforementioned MBSFN architecture is shown in Figure 14. The clear cells are part of the MBSFN area, while the shaded cells are excluded and they count as interference sources. The end users are only located in the center cell, while the other cells of the MBSFN area act as buffers to reduce the interference. This is called the *assisting ring* arrangement, and it is employed to reduce the interference at the edges of the MBSFN area. Note that the layout of Figure 14 models only one serving cell and one assisting ring, but many possibilities can be implemented, including irregularly shaped areas of many cells and multiple assisting rings. The performance achieved with MBSFN, both with and without the 5G extensions, has been investigated by considering a practical implementation envisaged within the FANTASTIC-5G EU H2020 project. The reference scenario instantiates an MBSFN network with one serving cell, containing the users, and two assisting rings around it, which are then surrounded by a ring of interfering cells. During the MBSFN sub-frames, the base stations of the MBSFN area transmit an HD video flow with a bit rate of 17 Mbps, therefore at the application layer, the model is the TraceBased. The mobility model is ConstantPosition while the scheduling algorithm is round-robin. The scenario is called f5g-uc6 because it models the use case 6 in the project's documentation and the command-line syntax to use it is:

```
./5G-air-simulator f5g-uc6 env isd density pattern time mcs harq (seed)
```

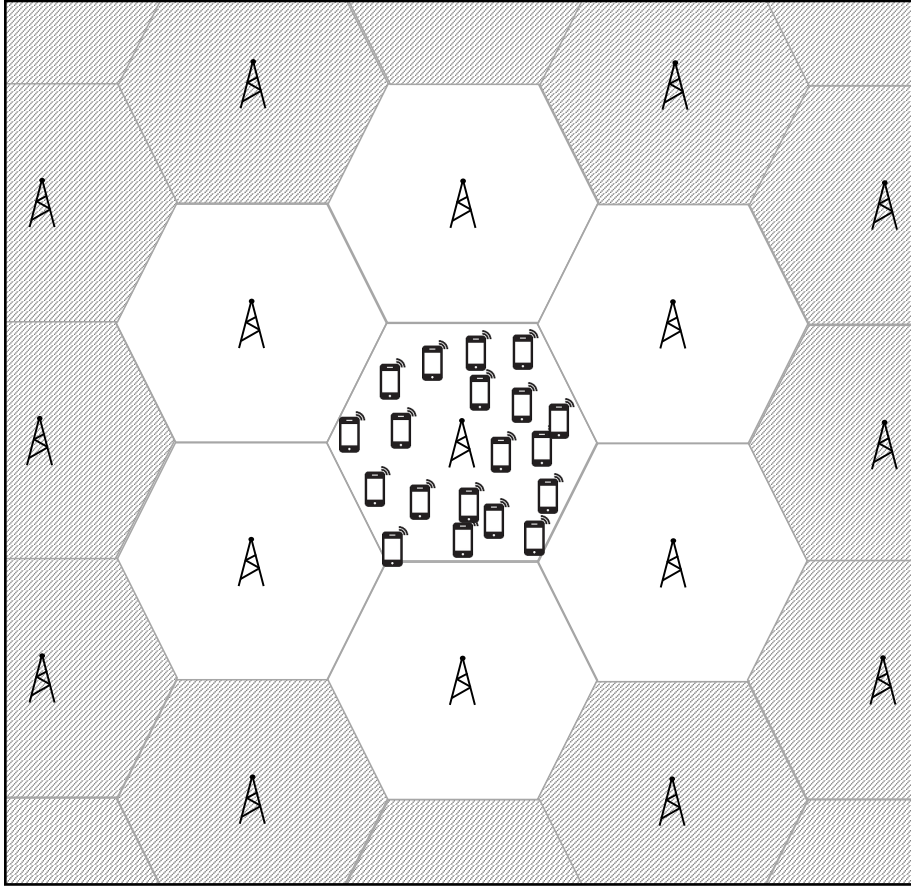


Figure 14: Scenario for multicast/broadcast use case evaluation.

where

- `env` is the propagation environment used for channel models, either "suburban" or "rural";
- `isd` is the ISD distance in km;
- `density` is the user density measured in users/km²;
- `pattern` is the number of sub-frames to reserve for MBSFN, from 0 to 6, where 0 disables MBSFN;
- `duration` is the duration in seconds of each simulation run;
- `mcs` is the MCS to use for transmission, it can be set to a fixed value from 0 to 28, or the value -1 can be used to enable the automatic selection based on CQI feedbacks;
- `harq` indicates whether to enable HARQ retransmission of broadcast packets or not, using the values 1 or 0, respectively;
- `seed` is an optional seed to initialize random quantities to different and reproducible values for each simulation run.

The performance of MBSFN and its 5G extensions is evaluated with the parameter settings shown in Table 9. Specifically, two main performance indicators have been considered: the cell-edge throughput at the application layer and the PLR. Figure 15 shows the Cumulative Distribution Function (CDF) plot from 0% to 5% for the considered scenarios, so that the cell-edge throughput values are at the top of the curves. The use of adaptive MCS with HARQ retransmis-

Table 9
Adopted Values for the Parameters of the Scenario

Parameter	Value
environment	suburban
isd	0.6 km
userDensity	400 users/km ²
mbsfnPattern	6
duration	10 s
mcs	16, 18, 20, -1
use_harq	1 with adaptive MCS, 0 otherwise
seed	1-30

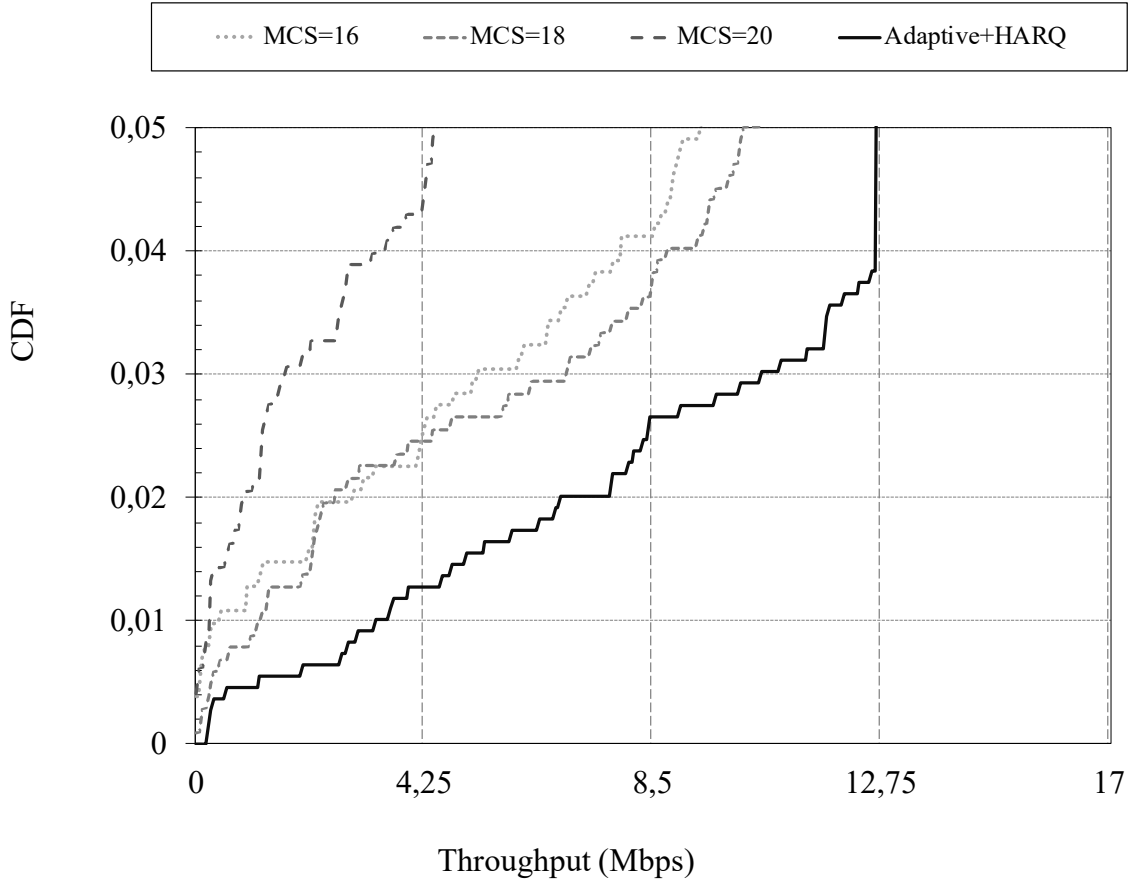


Figure 15: Cell-edge throughput at the application layer in the broadcast test.

sions allows more than 25% increase in cell-edge throughput compared to the best situation with a fixed MCS, while also avoiding the necessity to find the optimal value beforehand. Figure 16 shows the CDF plot for all the registered throughput values, also confirming previous results. As for the PLR, Table 10 shows the results of the simulations, demonstrating that the introduction of the new extensions added on top of MBSFN also reduce the PLR values compared to MBSFN alone. They also achieve a better trade-off between throughput and PLR, as the best configuration for cell-edge throughput of the baseline MBSFN is not the same as the best one in terms of PLR, but the adaptive solution is better than both of them at the same time.

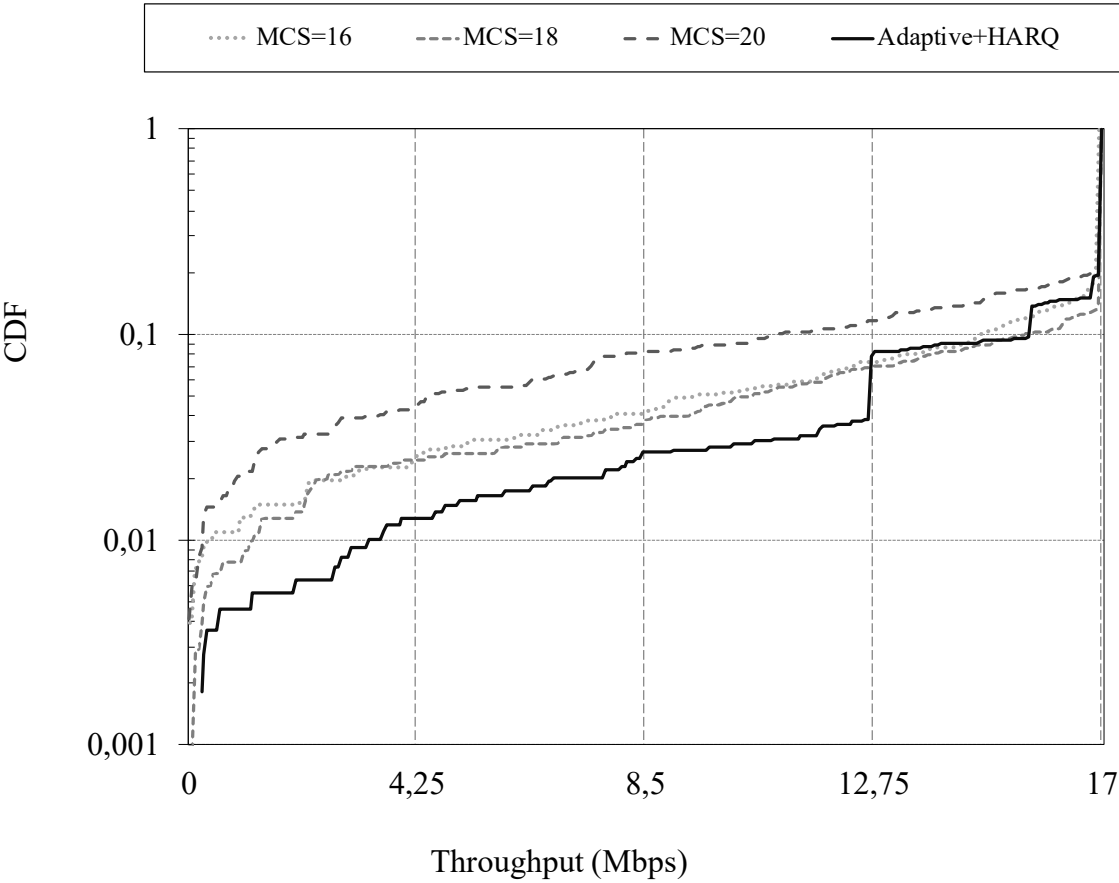


Figure 16: Throughput at the application layer in the broadcast test.

Table 10
PLR registered in broadcast test.

	Modulation and Coding Scheme (MCS)			
	16	18	20	Adaptive+HARQ
Average PLR (%)	7.3	5.1	9.0	3.3

7. High-speed environment and predictor antennas

When a mobile user is moving at a considerably high speed, such as 250 km/h or more, the quality of the radio link drops substantially (this can be the case of fast trains traveling long distances [22]). As expected, the reduced quality of the radio link results in a reduced capacity. Nevertheless, at the same time, it would be desirable to maintain a good Quality of Service (QoS) also in high-speed environments. Transmission schemes adopting predictor antennas emerged as a valuable technical component for achieving this goal in 5G.

7.1. Theoretical Description of the Technical Component

In general, one of the main causes of performance loss is the aging of the CSI between acquisition and utilization. The impact of this aging becomes disrupting in high-speed scenarios, where the channel quality rapidly changes also because of the interference originated by the Doppler spread. Without loss of generality, this section considers a challenging use case of interest for the 5G, which is a high-speed train. Here, the Separate Receive and Training

Antennas with Polynomial Interpolation (SRTA-PI) [22] emerged as a powerful technical component able to improve the connection quality by tackling the CSI aging phenomenon through an array of antennas deployed on top of the train. In other words, the train hosts a relay device offering wireless connectivity to passengers. According to the proposed technique, the antenna array samples the channel in different positions. Intermediate positions are obtained through interpolation of known positions so that the channel for the intended receiving antennas can be estimated with great accuracy despite the train's movement. For this reason, the antennas of the array act as predictor antennas [25]. Figure 17 shows the complete workflow for the SRTA-PI technique. During the training phase, the predictor antennas

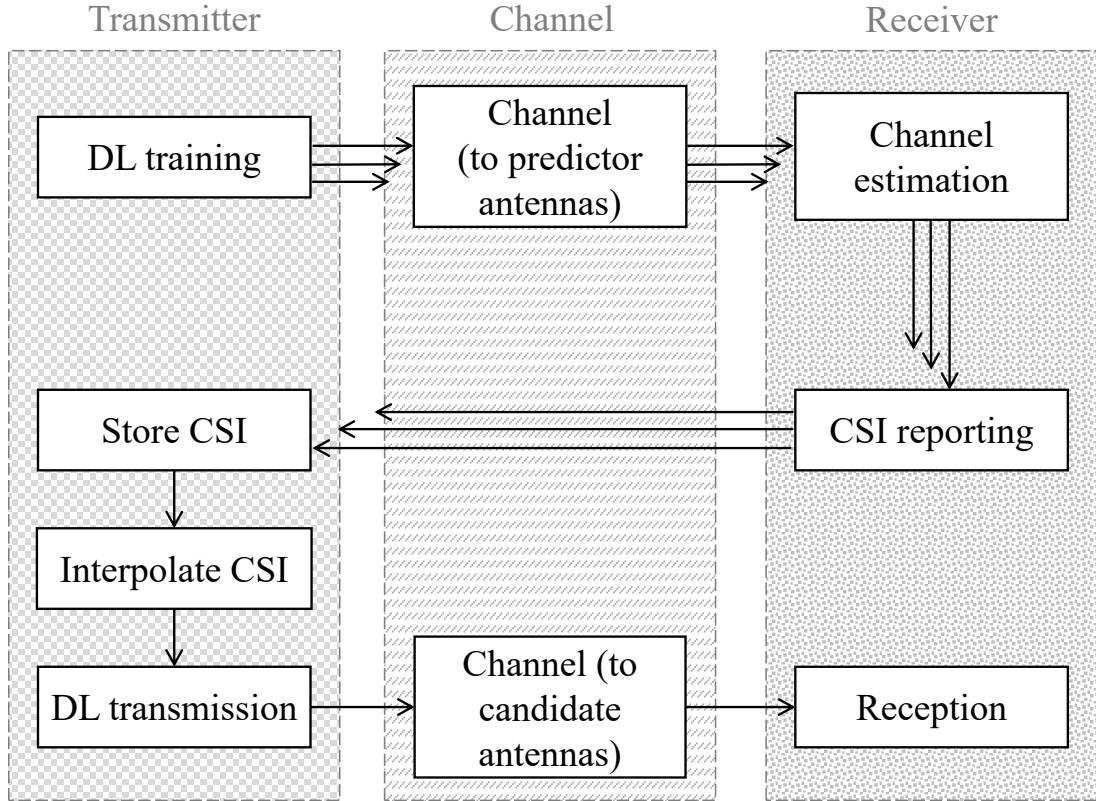


Figure 17: Block diagram of the SRTA-PI technique.

sample the channel and the receiver sends back those estimated samples to the base station during the CSI reporting phase. The base station stores the CSI obtained at regular intervals so that it can estimate the channel for any spatial position falling between the sampled positions by interpolation. By also knowing the position and speed of the receiver, it can determine the current position of the candidate receiving antennas and use the appropriate precoder.

7.2. Main implementation details

Table 11 summarizes the main functions related to the high-speed simulation scenarios. `Phy::SetSrtaPi()` sets the use of the SRTA-PI technique, that is disabled by default. It should be invoked for each device that adopts such a technique before the simulation is started. `Phy::SetWaveformType (Phy::WaveformType)` allows the selection of the waveform, to model Doppler spread interference. At the time of this writing, the selection is limited to OFDM, pulse-shaped OFDM, and an ideal waveform that is immune to Doppler spread. Doppler spread interference is then drawn from look-up tables as a function of the speed and the transmission power. Finally, the association between the signal and the corresponding channel realization is conducted in `DownlinkPacketScheduler::RBsAllocation()` and `UePhy::StartRx()`, for transmission and reception procedures, respectively.

Table 11

Main functions related to high speed simulations.

Key functionality	Class	Method	Parameters
Enable or disable the SRTA-PI technique for accurate channel estimation at thigh speeds.	Phy	SetSrtaPi()	flag to enable or disable SRTA-PI
Set the waveform type, which affect the amount of Doppler spread interference at high speeds.	Phy	SetWaveformType()	waveform type
Calculate the Doppler interference produced at a given speed and for a given waveform type.	Interference	ComputeDopplerInterference()	speed, waveform type
Receive a radio signal and calculate the SINR. With SRTA-PI enabled, consider the same channel realization for precoding and reception.	UePhy	StartRx()	packet burst, signal
Allocate resource blocks in the downlink. When using SRTA-PI, associate the transmitted signal with the channel realization used during precoding.	DownlinkPacketScheduler	RBsAllocation()	(none)

7.3. Reference Test and Results

The performance achieved with the aforementioned SRTA-PI technique has been investigated by considering a practical implementation envisaged within the FANTASTIC-5G EU H2020 project. Specifically, the network layout used to evaluate the SRTA-PI technique is shown in Figure 18. The reference scenario considers a train that moves on a straight horizontal line, with three-sectored base stations placed at both sides of the track in an hexagonal grid. There are two rows of base stations at each side, where the first one is used for service and the second one for modeling interference from the rest of the network. This layout is extended indefinitely by using wrap-around in the horizontal direction, so that movement can be extended for as long as needed without increasing the complexity. The mobile users are on the train, which acts as a relay station between them and the base stations. In this regard, the train can act as a single mobile user from the network's point of view, or as multiple users, depending on how many receiving units are installed. At the application layer, the model is the `InfiniteBuffer` while the mobility model is `LinearMovement`. The scenario is called `f5g-uc2` because it models the use case 2 in the project's documentation and the syntax used to perform the test is as follows:

```
./5G-air-simulator f5g-uc2 env isd nUe speed time nTx nM nRx sched
srta wfIdx (seed)
```

where

- `env` is the propagation environment used for channel models, either "suburban" or "rural";
- `isd` is the inter-site distance in km;
- `nUE` is the number of receiving units on the train;
- `speed` is the speed of the train in km/h;
- `time` is the duration in seconds of each simulation run;

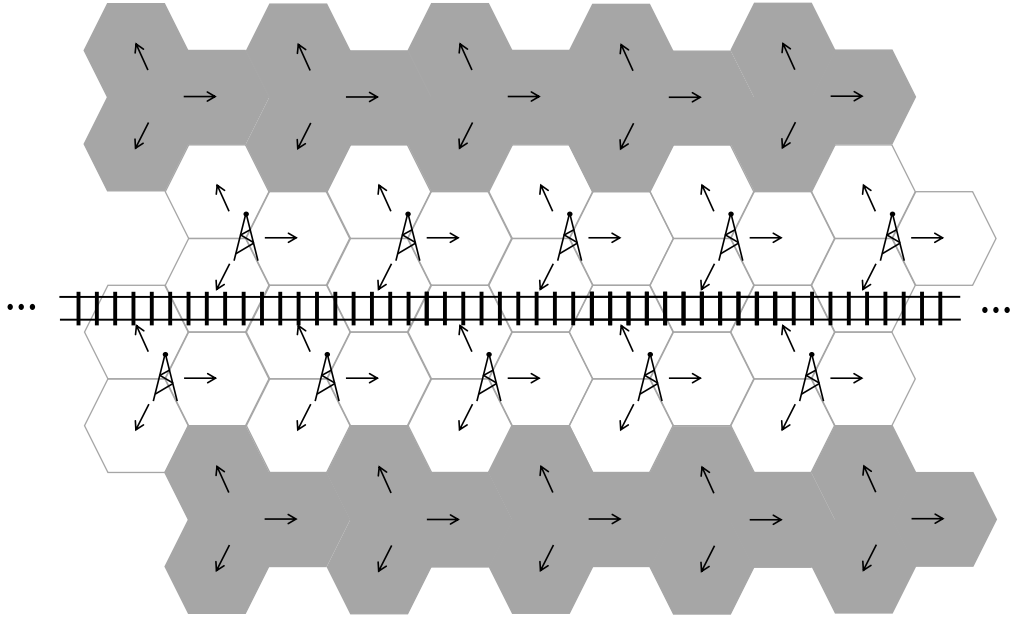


Figure 18: Reference scenario for the high-speed use case.

- n_{Tx} is the number of beams used at the base station for the first-stage precoding;
- n_M is the number of users that can be scheduled simultaneously for each resource block and TTI;
- n_{Rx} is the number of antennas used at each receiving unit, excluding predictor antennas;
- `sched` is the scheduling algorithm;
- `srta` indicates whether to enable SRTA-PI or not, using values 1 and 0 respectively;
- `wfIdx` indicates the waveform type to consider for Doppler spread calculation, where 0 is OFDM, 1 is pulse-shaped OFDM, and 2 is an ideal waveform without Doppler spread interference;
- `seed` is an optional seed to initialize random quantities to different and reproducible values for each simulation run.

The performance of the developed SRTA-PI technique is evaluated when the train is moving at different speeds, with different parameter settings, as reported in Table 12.

The most relevant outcome of this test is the cell throughput, which shows how SRTA-PI improves the overall performance, at the expense of greater complexity. The results obtained by either applying or not the SRTA-PI technique are shown in Figure 19. Results show that SRTA-PI can provide a throughput gain up to 100% at the highest speed compared to classic transmissions. However, the effect of Doppler spread still leaves a visible reduction of the performance at higher speeds.

8. The Enhanced Random Access Procedure

5G-air-simulator natively provides the support for the random access procedure, which endorses mobile terminals to establish a connection with the base station, without requiring any previously shared information. The presented version of the simulator supports both the baseline 5G contention-based random access procedure [50] and an enhanced procedure, as described in [26, 95].

Table 12

Adopted Values for the Parameters of the Scenario

Parameter	Value
environment	"suburban"
isd	0.5, 1, 2 km
nUE	8 receiving units
speed	30, 120, 250, and 500 km/h
time	(it depends on the speed, so that the distance traveled is always the same)
nTx	32 beams
nM	8 users
nRx	2 antennas
sched	round-robin
srtA	0, 1
wfIdx	0
seed	1-30

8.1. Theoretical Description of the Technical Component

The random access procedure is per se contention-based: since numerous users can access the shared channel at the same time, collisions may occur. The contention can be prevented, leading to a contention-free Random Access CHannel (RACH) procedure. Since this happens infrequently, a key aspect characterizing a RACH procedure is the contention resolution. The baseline 5G random access procedure standardized by 3GPP [96], which is initiated by the mobile terminal, is based on a 4-message handshake whose purpose is two-folded. Users achieve tight timing synchronization with the base station, on the one hand, and they receive an allocation grant of uplink resources, on the other. The first message can only be sent during a Random Access Opportunity, which is periodically scheduled by the base station. It consists of a preamble sequence, randomly chosen from a set of orthogonal sequences. The main goal of the preamble is to indicate the presence of an access request and to allow the base station to estimate the distance of the mobile terminal for the Timing Advance procedure. If two or more devices choose the same preamble during the same Random Access Opportunity, a collision occurs and the procedure may fail either immediately or at a later stage. Upon proper preambles detection, the base station sends back a Random Access Response (RAR) message. It consists of relevant information for each detected preamble, including the specific uplink resources to be used for sending the third message. If a collision is detected for a specific preamble, then the corresponding RAR will not be sent and the devices retry the procedure after a specific waiting time. Conversely, if a collision is unrecognized, two or more users will be assigned the same uplink resources and they will collide again on the third message, namely the Connection Request, that will be lost. Finally, after the successful delivery of the Connection Request, the base station replies with the last message, which is the Contention Resolution, also known as Msg4. When a device receives a Contention Resolution message addressed to it, the random access procedure is assumed to be completed. From this moment on, the successful devices can have reliable, collision-free communication with the base station. On the contrary, if the Msg4 is not properly received the Random Access Procedure has to be restarted.

As mentioned above, this procedure has been enhanced in [95], which emerged as a potential technical component for 5G systems. Specifically, after the base station performs the detection of preambles, it sends back a RAR containing multiple responses for each identified preamble, with different uplink resources assigned. Every mobile terminal which receives the RAR can randomly choose one of the uplink resources reserved for the preamble, selected during the first step. Thanks to this additional randomness, a collision over the selection of the preamble does not translate to a failure in the access procedure. This way, if two or more mobile terminals use the same preamble, they still have a chance to select a different resource assignment in the RAR and thus avoid the collision at the third step of the protocol. Basically, the multiple RARs act as multipliers for the number of preambles. The downside of this technique is that a correspondingly larger amount of uplink resources must be reserved for the transmission of Connection Request messages, which shrinks the resources available for actual user data.

Figure 20 summarizes the enhanced random access procedure.

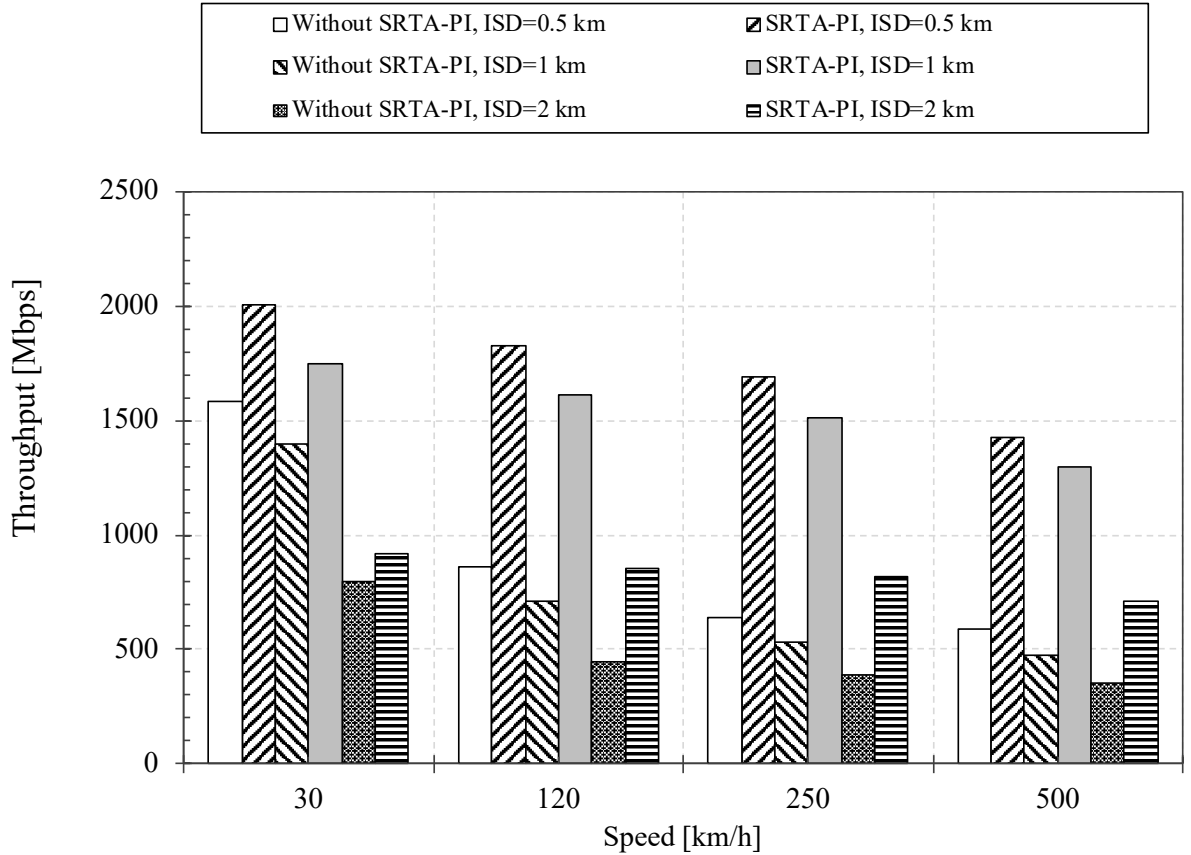


Figure 19: Throughput achieved in SRTA-PI test.

8.2. Main Implementation Details

Most of the random access features are summarized in Table 13.

Two different classes model the base station and the user general behavior, that are `GnbRandomAccess` and `UeRandomAccess`, respectively. Different random access procedure strategies are then selected thanks to `GnbRandomAccess::SetGnbRandomAccess` and `UeRandomAccess::SetUeRandomAccessType()` methods.

As for the user side, as soon as the application-layer traffic generator creates a packet, the user MAC entity starts the random access procedure immediately by calling the appropriate `StartRaProcedure()` method. On the other hand, the base station periodically scans all the preambles sent in RACH resources in order to find potential collisions. This is done through the `CheckCollisions()` method. In case of a preamble collision, the procedure fails for all the devices involved, which then need to call the `ReStartRaProcedure()` method. The latter is also in charge of verifying whether the maximum number of retry attempts has been reached, and in the affirmative case, it stops immediately the procedure. Conversely, the base station sends the second message to those devices that successfully completed the first message transmission. Lastly, the message flow advances until the procedure is properly complete, making the end-user active and able to transmit (or receive) data. In addition, the base station handles the RACH resources management by means of the `SetRachReservedSubChannels()` method. Specifically, if resources meet the configuration parameters, e.g., the periodicity, they are reserved for the RACH. Thus, end users are unable to exploit them to transmit regular data in the uplink, since only preambles can be transmitted. This control is performed during the uplink scheduling procedure by the method `isRachOpportunity()`. Finally, the constructors of the classes `GnbBaselineRandomAccess` and `GnbEnhancedRandomAccess` allow to control RACH resources occurrence, as well

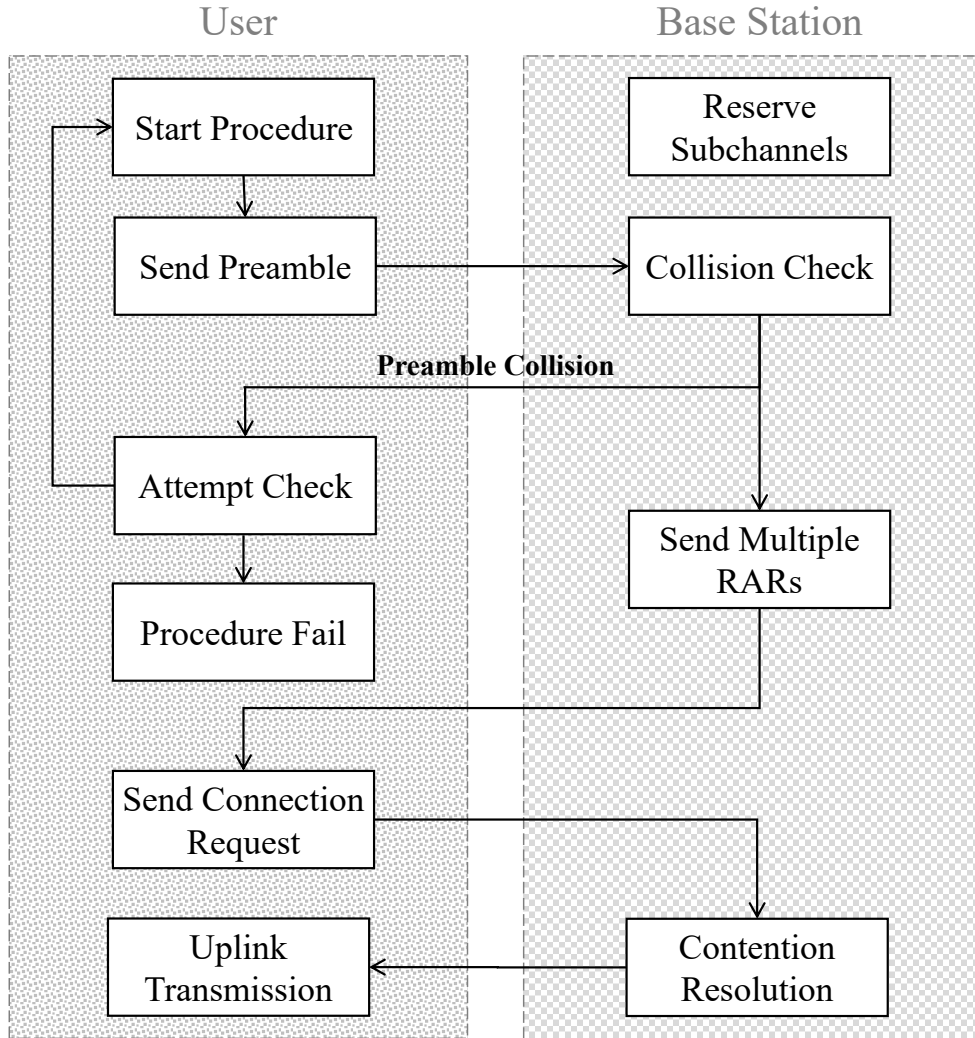


Figure 20: Block diagram of the enhanced random access procedure.

as the number of different preambles and the maximum number of retry attempts, among others.

8.3. Reference Test and Results

Conducted tests evaluated a reference mMTC scenario since a multitude of simultaneous transmissions brings to performance degradation in terms of preamble collisions during the random access procedure. It is then assumed a simple communication scheme, which is well suited to the low-cost requirements of MTC devices. The reference scenario is based on the SingleCell deployment, at the application layer the model is the CBR, while the mobility model is ConstantPosition. In particular, the activation time of the devices may be chosen either to follow a beta distribution with parameters (3,4) over a time interval of 10 s, or uniform distribution over a time interval of 5 s, hence modeling different event-driven transmission bursts. The users are positioned with a uniform random distribution over the simulated cell. As for the RACH configuration, one of the most common configurations has been chosen as a reference (RACH opportunities every 5 ms and 54 different congestion-free preambles). For the enhanced approach, the number of RARs transmitted for each preamble is set to 2 and 4. It is important to note that in case of collision, the procedure fails for all the involved devices, and can be repeated for a maximum of 3 times. The scenario is called MMC1 and the syntax used to perform the test is as follows:

Table 13

Main functions related to random access.

Key Functionality	Class	Method	Parameters
Choose the random access procedure strategy to use for the base station	GnbRandomAccess	SetGnbRandomAccessType()	Random access strategy
Choose the random access procedure strategy to use for users	UeRandomAccess	SetUeRandomAccessType()	Random access strategy
Determine if the timeout is expired	UeBaselineRandomAccess	checkRAProcedureTimeout()	(none)
Start the random access procedure	UeBaselineRandomAccess, UeEnhancedRandomAccess	StartRaProcedure()	(none)
Restart the random access procedure if the user is allowed to	UeBaselineRandomAccess, UeEnhancedRandomAccess	ReStartRaProcedure()	(none)
Reserve radio resources for RACH	GnbEnhancedRandomAccess, GnbBaselineRandomAccess	SetRachReservedSubChannels()	(none)
Verify whether sent preambles collided	GnbEnhancedRandomAccess, GnbBaselineRandomAccess	CheckCollisions()	(none)
Check whether radio resources have been reserved for RACH in current TTI	GnbEnhancedRandomAccess, GnbBaselineRandomAccess	isRachOpportunity()	(none)

```
./5G-air-simulator MMCI r nUe traf sched frStr maxD cbrI sync
type (seed)
```

where

- r is the cell radius
- nUe is the number of users in the cell (i.e., a given user density, depending on the value of r)
- $traf$ is the application layer traffic
- $frStr$ refers to the duplexing method
- $maxD$ is the maximum tolerable delay of the transmissions
- $cbrT$ is the time interval between two successive transmission by the same user
- $sync$ is used to determine whether users transmits synchronously or not
- $type$ is the random access procedure strategy, 1 for the baseline and 2 for the enhanced procedure
- $seed$ is an optional seed to initialize random quantities to different and reproducible values for each simulation run

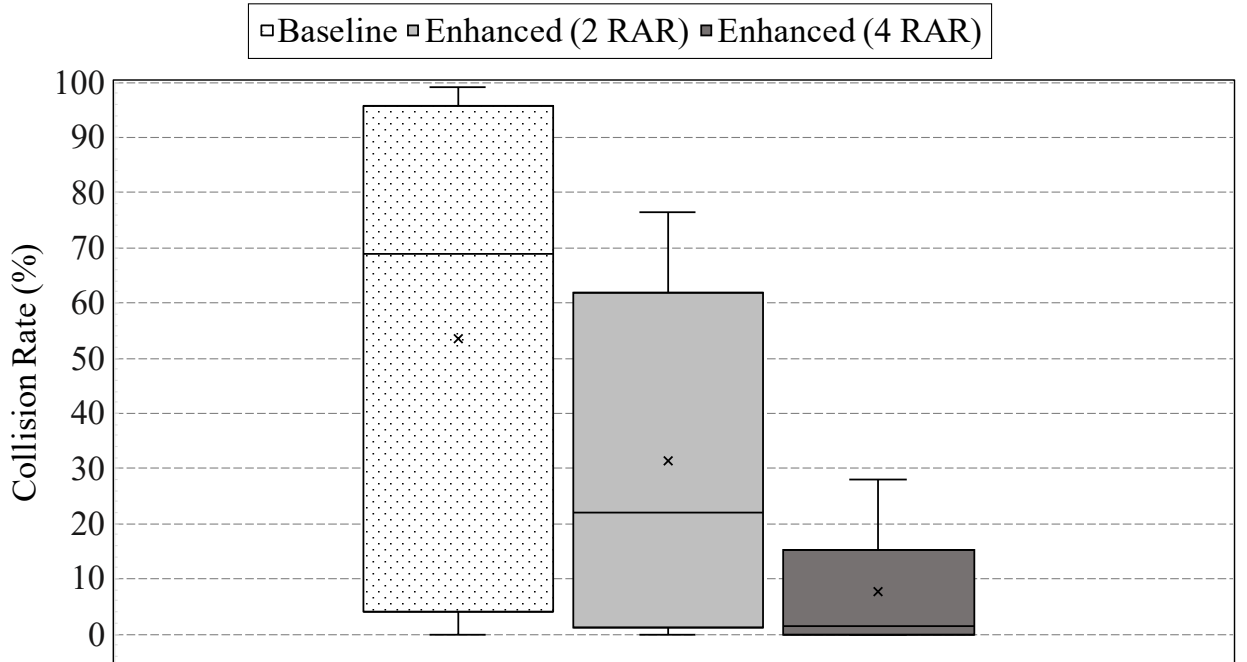
The performance is evaluated with different parameter settings, as reported in Table 14.

Baseline results investigate the collision rate of the random access process. Figure 21 shows the collision rate for each approach of interest. The figure highlights the collision rates, their centroids (i.e., the small crosses), the 25th and the 75th percentile (i.e., the bottom line and the top line of the rectangles), as well as the minimum and the maximum measured value (i.e., the edges of the vertical lines). The most noticeable feature is the incredibly high collision rate of the baseline random access. In this case, almost no preambles can be detected, and the devices retry connection until they succeed or fail. In contrast, the 5G enhanced approach with 4 RARs experiences only 28% collision rate at most, proving the effectiveness of the enhanced approach.

Table 14

Adopted Values for the Parameters of the Scenario

Parameter	Value
r	290 m
nUe	156000 (10^6 UE/km ²)
traf	CBR
frStr	FDD
maxD	10 s
cbrT	300 s
sync	"sync"
type	0, 1
seed	1-50

**Figure 21:** Comparison between the obtained preamble collision rates

9. NarrowBand-Internet of Things

NB-IoT is a cellular radio access technology addressing the needs of low data rate devices massively deployed within a cell. It requires a small bandwidth to properly work and it can be efficiently implemented in already existing cellular technologies. Therefore, it is usually regarded as a promising standard to meet the requirements of the future 5G development for the IoT. Accordingly, *5G-air-simulator* provides the support for a variety of NB-IoT features.

9.1. Theoretical Description of the Technical Component

An NB-IoT carrier requires a 180 kHz bandwidth in downlink and uplink [97], where Orthogonal Frequency Division Multiple Access (OFDMA) and Single-Carrier Frequency Division Multiple Access (SC-FDMA) are used as multiple access methods, respectively. Besides, other carriers may be used to supply a higher bandwidth. Fundamentals NB-IoT feature are the partitioning into coverage classes and repetitions. Up to three coverage class may be configured in a cell, in order to serve devices experiencing different received power levels. Furthermore, different system configurations can be deployed in a single NB-IoT cell, each tied to a particular coverage class. For instance, during the random access procedure, users have different preamble transmission attempts in each coverage class [28].

As for the repetitions, this technique can be used for coverage extension, lengthening the duration of the transmissions. Simplistically, coverage enhancement is achieved by trading off data rate through increasing the number of transmission repetitions. NB-IoT also introduced the flexible numerology, at least in the uplink direction, for better accommodating different device requirements. As a consequence, an additional subcarrier spacing of 3.75 kHz is supported, as well as the traditional spacing of 15 kHz. Nevertheless, uplink flexible numerology significantly alters the radio resource structure. The new baseline NB-IoT uplink radio resource, namely Resource Unit (RU), is the smallest unit to map a transport block [98]. It is assigned to a single user only. An RU depends on the supported uplink configurations, that are *Single-Tone* and *Multi-Tone*. *Single-Tone* uses either 3.75 or 15 kHz subcarrier spacing and each subcarrier represents an RU. As a result, a 180 kHz carrier is divided in either 48 or 12 RUs, respectively. Contrarily, when *Multi-Tone* configuration is applied, the subcarrier spacing can be 15 kHz solely. However, 3, 6 or 12 adjacent subcarriers may concur to form a single RU. According to the subcarrier spacing and the number of tones per RU, its duration changes accordingly [99] NB-IoT uplink scheduling techniques must take into account whether *Single-Tone* or *Multi-Tone* transmission is used. Moreover, the MAC scheduler does not only choose how to assign radio resources for the current TTI but also for following instants, since RUs are time-multiplexed [27]. This greatly complicates scheduling decisions because the base station should know which RUs, and how many of them, have been assigned to each user both at present and in the future.

9.2. Main Implementation Details

In a mMTC context, when a massive number of devices typically sends data, the uplink direction generally deserves more attention than the downlink. Accordingly, NB-IoT main novelties focus on the uplink direction, where the channel is more congested. For the same reason, the *5G-air-simulator* implements only the NB-IoT uplink side. Figure 22 shows a high-level illustration of the main features implemented in the simulator, whereas Table 15 summarizes the related code. Essentially, the *BandwithManager*, *nb-AMModule* and *nbUplinkPacketScheduler* classes provide

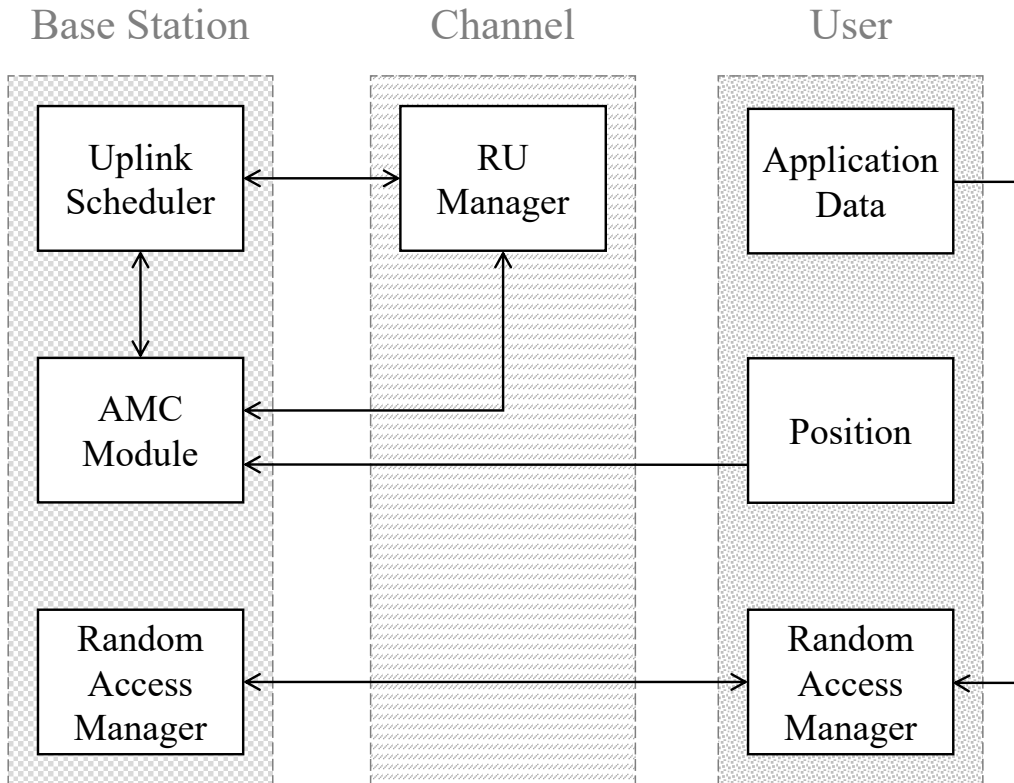


Figure 22: Block diagram of main implemented NB-IoT features

Table 15

Main functions related to NB-IoT features.

Key Functionality	Class	Method	Parameters
Generate NB-IoT carriers and sub-channels	BandwidthManager	CreateNbIoTspectrum()	Number of carriers, subcarrier spacing, number of tones
Determine the maximum number of carriers available for NB-IoT depending on the chosen reference bandwidth.	BandwidthManager	GetMaxNbIoTcarriers()	(none)
Get the usable resource blocks for NB-IoT implementation.	BandwidthManager	GetNbIoTrb()	(none)
Apply the correct RU duration.	FrameManager	setTTILength()	number of tones, subcarrier spacing
Get the proper number of RUs needed to transmit a packet.	nb-AMCModule	GetNbOfRUsFromSize()	MCS index, packet size
Get the TBS related to a specific MCS index and number of RUs.	nb-AMCModule	GetTBSfromMCS()	mcs index, RU index
Get the proper number of RUs needed to transmit a packet.	nb-AMCModule	GetMCSfromDistance()	Distance from base station, cell radius, number of tones
Start the uplink scheduling procedure for NB-IoT devices.	nbUplinkPacketScheduler	DoSchedule()	(none)
Perform the RU assignment for scheduled users following the Round Robin algorithm.	nbRoundRobinUplinkPacketScheduler	RUsAllocation()	(none)
Perform the RU assignment for scheduled users according to a FIFO strategy.	nbFifoUplinkPacketScheduler	RUsAllocation()	(none)

the support for NB-IoT features. *BandwidthManager* deals with multiple carriers, subcarrier spacings, *Single-Tone* and *Multi-Tone* transmissions; the latter can be configured for using either 3, 6 or 12 tones. The AMC module, namely *nbAMCModule*, picks the appropriate TBS, starting from the selected MCS index and number of RUs given by the chosen scheduling strategy. The flexible structure of an uplink RU greatly complicates the radio resource management. As a consequence, MAC schedulers should carefully consider the different RU lengths when performing resource assignments. The length of a RU can be set via the *FrameManager::setTTILength()* method. Essentially, it gives the correct length of the TTI, based on the chosen numerology.

According to what has been previously stated, the scheduling paradigm is redesigned. To this purpose, the abstract class *nbUplinkPacketScheduler* provides inherent methods of all the scheduling strategies. Then, two different scheduler classes have been developed, related to two well-known strategies: First-In First-Out (FIFO) and Round-Robin (RR). It is important to observe that additional scheduling algorithms can also be developed following the same rationale.

9.3. Reference Test and Results

A first evaluation has been conducted to fulfill a preliminary performance assessment of the NB-IoT technical component. The reference scenario is based on the *SingleCell* deployment, at the application layer the model is the CBR, while the mobility model is *ConstantPosition*. The users are positioned with a uniform random distribution over the simulated cell. The scenario is called *nbCell* and the command-line syntax to use it is:

```
./5G-air-simulator nbCell sched time r nUe bw nC spa tones cbrT
cbrS aMax nCl [p0] [pAtt] [pRep] [rWind] [nP] [period] [o] [boW] (seed)
```

where

- `sched` is the scheduling algorithm;
- `time` is the duration in seconds of each simulation run;
- `r` is the cell radius;
- `nUe` is the number of users in the cell;
- `bw` is the total bandwidth used by the base station;
- `nC` is the number of NB-IoT carriers;
- `spa` is the subcarrier spacing;
- `tones` is the number of tones;
- `cbrT` is the time interval between two successive transmission by the same user;
- `cbrS` is the size of the data sent by the users at each transmission;
- `aMax` is the maximum number of retry attempts for the random access procedure;
- `nCl` is the number of the coverage classes;
- `[p]` is the probability that users belong to the coverage classes;
- `[pA]` is the number of preamble transmission attempts;
- `[pRep]` is the number of preamble repetition;
- `[rWind]` is the duration of the RAR window;
- `[nP]` is the number of different RACH preambles;
- `[period]` is the periodicity of RACH resources;
- `[o]` is the starting time of RACH resources;
- `[boW]` is the duration of the RACH backoff window;

Conducted tests demonstrated the impact of the average number of transmission requests per second, λ , on a reference NB-IoT network, with the parameter settings shown in Table 16.

System performance was evaluated in terms of average cell goodput and end-to-end packet delays. Figure 23 shows the average system goodput, demonstrating how Single-Tone mode is indeed capable of handling a higher number of transmission requests. In fact, more users can be scheduled at the same time during a TTI compared to the Multi-Tone configuration. It is important to note that the results do not follow a monotonic behavior: moving from $\lambda = 40$ to $\lambda = 60$, the network registers a performance degradation. This is not caused by radio channel errors (which are not implemented yet), but it is due to the limited number of mobile terminals that completed the random access procedure.

Lastly, Table 17 shows the statistics of the end-to-end packet delays when Single-Tone configuration is used and a subcarrier spacing equal to 15 kHz is applied. Delays are calculated by considering the influence of random access procedure, scheduling decisions, and the actual physical transmission. The most noticeable feature is that packet delays grow with λ . Indeed, when λ increases more users perform the random access procedure and the amount of time needed to complete it increases as well. At the same time, for λ values greater than 20, the difference between scheduling policies becomes more noticeable. In particular, RR guarantees lower delays with respect to FIFO for most of the users.

Table 16

Adopted Values for the Parameters of the Scenario

Parameter	Value
sched	FIFO, Round-Robin
time	150 s
r	1000 m
nUe	1200, 2400, 3600 users
bw	5 MHz
nC	1 carrier
spa	3.75, 15 kHz
tones	1, 3, 12
cbrT	60 s
cbrS	256 Bytes
aMax	4 Attempts
nCl	1 coverage class
[p]	1 (100%)
[pA]	3 attempts
[pRep]	1 repetition
[rWind]	12 ms
[nP]	48 preambles
[period]	320 ms
[o]	8 ms
[boW]	256 ms
seed	1-50

Table 17

5th percentile, median, and 95th percentile of the end-to-end packet delay (in seconds)

	λ [requests/s]		
	20	40	60
FIFO	0.2, 0.5, 1.1	1.0, 5.2, 10.6	0.7, 3.7, 66.7
RR	0.2, 0.5, 1.1	0.8, 4.1, 19.9	0.7, 3.3, 65.6

10. Performance Testing

Several simulations have been executed to assess the performance of the scenarios of the presented 5G technical components, as well as some of the fundamental network deployments described in Section 4.1.2. Simulations ran using a consumer notebook with a Quad-Core Intel Core i5 @2.3 GHz and 8 GB of RAM for accurately reproducing the performance experienced by an average user. Table 18 shows the obtained time performance. The simulator runs without critical issues and with decent execution time even on common machines, although performance may prominently increase with the usage of more powerful computers. Reported results clearly demonstrates that *i*) simple scenarios can be simulated in a very limited amount of time, and *ii*) complex scenarios (i.e., those with many users, base stations, and cells, as well as those implementing technical components requiring the implementation of many functionalities) inevitably register a higher computational complexity. However, by considering the complexity of these latter group of scenarios, the ratio between the real time and the simulation time still remains within an acceptable range of values.

It is important to note that, since the presented simulation framework is a single-threaded software, several concurrent instances may be executed by exploiting CPUs' multithreading, hence enabling a substantial performance enhancement in case of a numerous set of simulations to be executed.

11. What's Next

5G-air-simulator can be leveraged as a valid open-source instrument to model and analyze the 5G air interface. Furthermore, given both the open-source nature of the tool introduced in this paper and its modularity, any new tech-

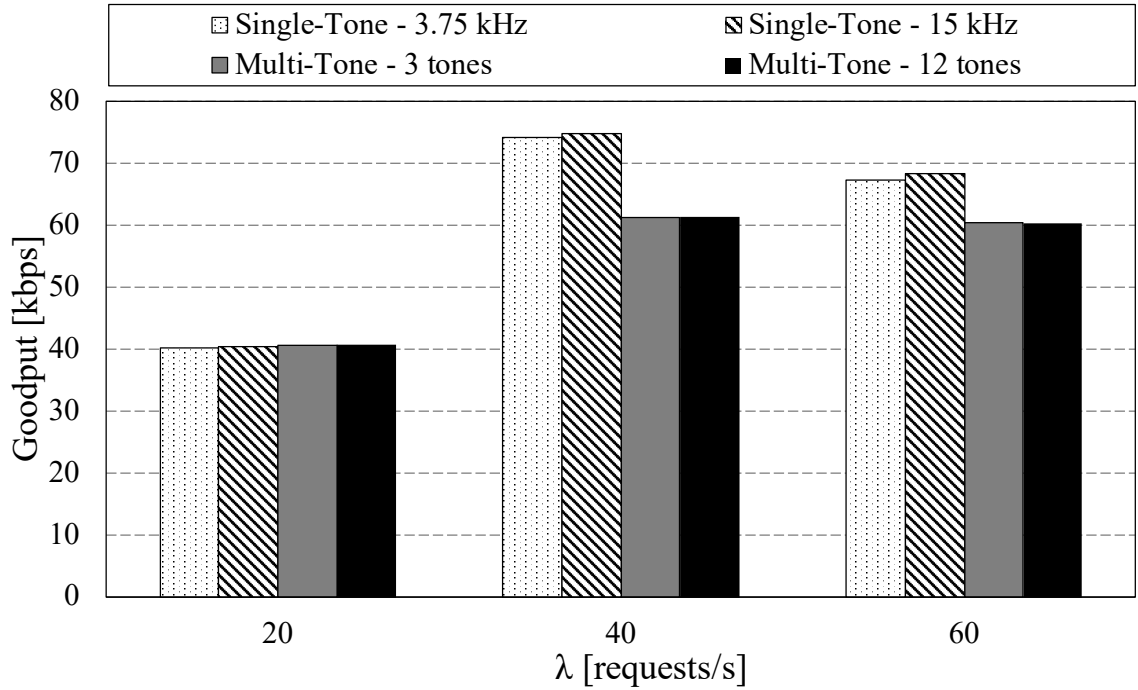


Figure 23: Average Cell Goodput

Table 18

Performance testing of 5G-air-simulator.

Scenario	Simulation Time [s]	Real Time [s]	Real Time/ Simulation Time
SingleCell	25	30	1.20
SingleCellWithInterference	46	27	0.59
MultiCell	100	711	7.11
SingleCellWithFemto	30	547	18.23
f5g-uc1 (mMIMO) - 104 UE (Rural)	10	3714	371.40
f5g-uc1 (mMIMO) - 150 UE (Suburban)	10	4510	451.00
f5g-uc1 (mMIMO) - 104 UE (Urban)	10	3808	380.80
f5g-uc6 (Extended Multicast)	10	2028	202.80
f5g-uc2 (High-speed)	6	1397	232.83
MMC1 (Enhanced Random Access) - 1560 UE	11	1	0.09
MMC1 (Enhanced Random Access) - 156000 UE	15	3357	223.80
nbCell1 (NB-IoT) - 1200 UE	150	55	0.37
nbCell1 (NB-IoT) - 3600 UE	150	993	6.62

nical components may be integrated in order to pave the way for different research directions. Technical components to be included in the 5G-air-simulator are listed (but not limited to) below:

- **Ultra-Reliable Low-Latency Communications (URLLC)** will facilitate several new services and verticals, ranging from Tactile Internet to vehicle platooning and autonomous driving. Nevertheless, these applications rise tricky challenges in terms of latencies, reliability, availability, and security [100, 101], hence requiring further investigations. The FrameManager class is the most important class to extend in order to support this technical component, for taking care of the different time structure of radio resources. Moreover, the introduction of pre-emption based puncturing in the DownlinkPacketScheduler class is foreseen.

- **Unmanned Aerial Vehicles (UAVs)** play an important role in 5G wireless technologies [102]. On the one hand, UAVs may be leveraged in intelligent heterogeneous architecture for enhancing cells' capacity or providing network service recovery [103]. On the other hand, thanks to the capabilities offered by the NR, it is possible to realize large-scale UAVs deployment, hence presenting new research challenges as well as opportunities [104]. For the support of UAVs in the *5G-air-simulator*, it is essential to develop new 3D mobility and radio channel models [105], as well as new network deployments for the envisioned heterogeneous architectures.
- **D2D** communication emerged as a key technical component to offload the traffic from cellular networks exploiting direct links. Sidelink communication indeed reduces the computational complexity at the base station and enhances the cell's capacity. Even though few basic D2D features have been standardized for 4G, they are currently under discussion in 3GPP, specifically for enhanced-V2X services[106]. However, a number of challenges and research directions are still open [107]. The main classes interested in the integration of this technical component are `Ue` and `PacketScheduler`, for carrying out autonomously the operations normally controlled by the base station, such as resource allocation and subsequent data transmissions.
- **Radio Access Network Slicing** notably improves the end-to-end performance, thanks to the flexibility introduced in NR and the virtualization of the network [108]. Moreover, Network Slicing allows the splitting and the configuration of radio resources to properly serve users with a given QoS profile. The lifecycle of slices and the necessary management tasks have been already discussed by 3GPP [109] and many research activities are being conducted on this topic [110]. Still, Radio Access Network Slicing remains at an early stage in terms of its development [111]. Overall, the `DownlinkPacketScheduler` and `UplinkPacketScheduler` should be the primary classes to be extended for managing different radio slices. At the same time, it is utterly important to provide the support to Bandwidth Parts and numerology multiplexing in the classes `BandwidthManager` and `AMCModule`, as well as a `FrameManager` extension to support different numerologies in different subframes.
- **mmWave** communications, which are currently under investigation of the 3GPP [50], have become increasingly important for their ability to provide high-throughput and low-latency. They extensively exploit large antenna arrays and adaptive beamforming to achieve highly directional transmissions. However, this approach has a disruptive impact not only on the physical layer but also on the other layers of the protocol stack, hence affecting several features, such as cell search, broadcast signaling, random access, etc. [112]. For this reason, the design of mmWave 5G systems still requires considerable research efforts [8]. For the support of mmWave communications, it is important to properly integrate new channel models in the class `ChannelRealization`, as well as to add extended-bandwidth features in `BandwidthManager` and `AMCModule`.

In parallel, future work includes a number of new supporting models in order to enhance the present technical components and enabling future ones. Several enhancements may include Bandwidth Parts, a `FrameManager` extension to support different numerologies in different subframes, HARQ activation/deactivation per flow, new handover procedures, Massive MIMO in the uplink direction, an extension of the NB-IoT module with downlink transmissions, repetitions, peculiar channel models and in-band coexistence with 5G, as well as Supplementary Uplink, and the introduction of the new 5G Service Data Adaptation Protocol (SDAP).

12. Conclusions

In this tutorial paper, we have deeply presented an open-source simulation framework for the 5G air interface, *5G-air-simulator*, as an instrument to study a number of technical components already standardized by the 3GPP, under investigation by other standardization entities, or discussed in the scientific literature. The developed simulation framework inherits the core functionalities from the worldwide known LTE-Sim tool and integrates additional features and many new technical components, such as new models for channel propagation and data transmission, MIMO and Massive MIMO transmission modes, extended multicast/broadcast operation, predictor antennas, enhanced random access procedure, and NB-IoT. The code, which is already publicly available [16], will provide a sound basis for researchers prone to develop their own modules to test additional groundbreaking 5G features. For this reason, in addition to the framework description and discussion, this tutorial intended to educate any researcher that plans to use the simulator by providing a step-by-step comprehensive guide to carry out simulations and obtain representative KPIs. Specifically, a brief description of *5G-air-simulator*'s general properties is provided, explaining the new features introduced since the last public release of LTE-Sim, concentrating on new models for channel propagation and data

transmission. We have also focused on a series of simulation campaigns for typical 5G application scenarios, with a single and organic point of view, providing at the same time a functional theoretical description and the main implementation details. Finally, we broadly describe the new technical components to be included in the *5G-air-simulator*, to provide further insight into the future work as well as to demonstrate how to exploit the flexibility of the proposed open-source framework.

Acknowledgments

This work was supported by the PRIN project no. 2017NS9FEY entitled “Realtime Control of 5G Wireless Networks: Taming the Complexity of Future Transmission and Computation Challenges” funded by the Italian MIUR. It has been also partially supported by the Italian MIUR PON projects Pico&Pro (ARS01_01061), AGREED (ARS01_00254), FURTHER (ARS01_01283), RAFAEL (ARS01_00305), and by Apulia Region (Italy) Research projects E-SHELF (OSW3NO1) and INTENTO (36A49H6).

List of Acronyms

3GPP	3 rd Generation Partnership Project
4G	4 th Generation
5G	5 th Generation
AM	Acknowledged Mode
AMC	Adaptive Modulation and Coding
ARQ	Automatic Repeat reQuest
BLER	Block Error Rate
BMS	Broadcast/Multicast Services
BWP	BandWidth Part
CDF	Cumulative Distribution Function
CQI	Channel Quality Indicator
CSI	Channel State Information
D2D	Device-to-Device
ECDF	Empirical Cumulative Distribution Function
eMBB	Enhanced Mobile Broadband
FDD	Frequency Division Duplex
FEC	Forward Error Correction
FIFO	First-In First-Out
HARQ	Hybrid Automatic Repeat reQuest
IoT	Internet of Things
ISD	Inter-Site Distance
JSDM	Joint Spatial Division and Multiplexing
KPI	Key Performance Indicator
L2S	Link-To-System
LTE	Long Term Evolution
LTE-A	LTE-Advanced
MAC	Media Access Control
MBSFN	Multicast Broadcast Single Frequency Network
MCS	Modulation and Coding Scheme
MIESM	Mutual Information Effective SINR Mapping
MIMO	Multiple-Input Multiple-Output
mMTC	Massive Machine-Type Communications
MRC	Maximum Ratio Combining

MTC	Machine-Type Communication
NB-IoT	NarrowBand IoT
NR	New Radio
OFDM	Orthogonal Frequency Division Multiplexing
OFDMA	Orthogonal Frequency Division Multiple Access
PDCP	Packet Data Convergence Protocol
PLR	Packet Loss Ratio
PMI	Precoding Matrix Indicator
QoS	Quality of Service
RACH	Random Access CHannel
RAR	Random Access Response
RB	Resource Block
RI	Rank Indicator
RLC	Radio Link Control
RR	Round-Robin
RU	Resource Unit
RZF	Regularized Zero-Forcing
SC-FDMA	Single-Carrier Frequency Division Multiple Access
SDAP	Service Data Adaptation Protocol
SINR	Signal to Interference plus Noise Ratio
SRTA-PI	Separate Receive and Training Antennas with Polynomial Interpolation
TBS	Transport Block Size
TDD	Time Division Duplex
TM	Transparent Mode
TM	Transmission Mode
TTI	Transmission Time Interval
UAV	Unmanned Aerial Vehicle
UM	Uncknowledged Mode
URLLC	Ultra-Reliable Low-Latency Communications
V2X	Vehicular to Everything
VoIP	Voice over IP

References

- [1] N. Alliance, 5G White Paper, Next Generation Mobile Networks, White paper (2015).
- [2] 3GPP, Study on New Radio Access Technology Physical Layer Aspects (Release 14), Technical Report 38802, 3rd Generation Partnership Project, 2017.
- [3] F. Schaich, B. Sayrac, M. Schubert, H. Lin, K. Pedersen, M. Shaat, G. Wunder, A. Georgakopoulos, FANTASTIC-5G: 5G-PPP Project on 5G air interface below 6 GHz, in: European Conference on Network and Communications, 2015.
- [4] Y. Wang, J. Xu, L. Jiang, Challenges of system-level simulations and performance evaluation for 5G wireless networks, *IEEE Access* 2 (2014) 1553–1561.
- [5] S. Cho, S. Chae, M. Rim, C. G. Kang, System level simulation for 5G cellular communication systems, in: Ubiquitous and Future Networks (ICUFN), 2017 Ninth International Conference on, IEEE, 2017, pp. 296–299.
- [6] I.-P. Belikaidis, A. Georgakopoulos, E. Kosmatos, I. de-la Bandera, D. Palacios, R. Barco, P. Demestichas, 5G Component Carrier Management Evaluation by Means of System Level Simulations, in: 2019 European Conference on Networks and Communications (EuCNC), IEEE, 2019, pp. 592–596.
- [7] M. Liu, P. Ren, Q. Du, W. Ou, X. Xiong, G. Li, Design of system-level simulation platform for 5G networks, in: Communications in China (ICCC), 2016 IEEE/CIC International Conference on, IEEE, 2016, pp. 1–6.
- [8] M. Mezzavilla, M. Zhang, M. Polese, R. Ford, S. Dutta, S. Rangan, M. Zorzi, End-to-end simulation of 5g mmwave networks, *IEEE Communications Surveys & Tutorials* 20 (2018) 2237–2263.
- [9] N. Patriciello, S. Lagen, B. Bojovic, L. Giupponi, An e2e simulator for 5g nr networks, *Simulation Modelling Practice and Theory* 96 (2019) 101933.
- [10] M. K. Müller, F. Ademaj, T. Dittrich, A. Fastenbauer, B. R. Elbal, A. Nabavi, L. Nagel, S. Schwarz, M. Rupp, Flexible multi-node simulation of cellular mobile communications: the Vienna 5G System Level Simulator, *EURASIP Journal on Wireless Communications and Networking* 2018 (2018) 227.

- [11] M. Han, J. W. Lee, C. G. Kang, M. J. Rim, 5g k-simsys: Open/modular/flexible system level simulator for 5g system, in: 2018 IEEE International Symposium on Dynamic Spectrum Access Networks (DySPAN), IEEE, 2018, pp. 1–2.
- [12] Tetcos, NetSim-Network Simulator & Emulator, 2019. URL: <https://www.tetcos.com/>, [Online; Accessed 10 Oct. 2019].
- [13] C.-K. Jao, C.-Y. Wang, T.-Y. Yeh, C.-C. Tsai, L.-C. Lo, J.-H. Chen, W.-C. Pao, W.-H. Sheen, Wise: a system-level simulator for 5g mobile networks, IEEE Wireless Communications 25 (2018) 4–7.
- [14] S. Martiradonna, A. Grassi, G. Piro, G. Boggia, 5g-air-simulator: An open-source tool modeling the 5g air interface, Computer Networks 173 (2020) 107151.
- [15] F. Boccardi, R. W. Heath, A. Lozano, T. L. Marzetta, P. Popovski, Five Disruptive Technology Directions for 5G, IEEE Communications Magazine 52 (2014) 74–80.
- [16] 5G-air-simulator Official Repository, 2020. URL: <https://github.com/telematics-lab/5G-air-simulator>, [Online; accessed 30-March-2020].
- [17] G. Piro, L. A. Grieco, G. Boggia, F. Capozzi, P. Camarda, Simulating LTE cellular systems: An open-source framework, IEEE transactions on vehicular technology 60 (2011) 498–513.
- [18] F. Capozzi, G. Piro, L. A. Grieco, G. Boggia, P. Camarda, Downlink packet scheduling in lte cellular networks: Key design issues and a survey, IEEE Communications Surveys & Tutorials 15 (2013) 678–700.
- [19] 3GPP, Evolved Universal Terrestrial Radio Access (E-UTRA); Further advancements for E-UTRA physical layer aspects, Technical Report 36814, 3rd Generation Partnership Project, 2010.
- [20] E. G. Larsson, O. Edfors, F. Tufvesson, T. L. Marzetta, Massive mimo for next generation wireless systems, IEEE communications magazine 52 (2014) 186–195.
- [21] B. Mouhouche, M. Al-Imari, Optimization of delivery time in broadcast with acknowledgement and partial retransmission, in: Broadband Multimedia Systems and Broadcasting (BMSB), 2016 IEEE International Symposium on, IEEE, 2016, pp. 1–5.
- [22] D.-T. Phan-Huy, M. Sternad, T. Svensson, Making 5G adaptive antennas work for very fast moving vehicles, IEEE Intelligent Transportation Systems Magazine 7 (2015) 71–84.
- [23] A. Laya, L. Alonso, J. Alonso-Zarate, Is the random access channel of lte and lte-a suitable for m2m communications? a survey of alternatives., IEEE Communications Surveys and Tutorials 16 (2014) 4–16.
- [24] Y.-P. E. Wang, X. Lin, A. Adhikary, A. Grovlen, Y. Sui, Y. Blankenship, J. Bergman, H. S. Razaghi, A primer on 3gpp narrowband internet of things, IEEE Communications Magazine 55 (2017) 117–123.
- [25] A. Grassi, G. Piro, G. Boggia, D.-T. Phan-Huy, A system level evaluation of SRTA-PI transmission scheme in the high-speed train use case, in: Proc. of IEEE International Conference on Telecommunications (ICT), Saint-Malo, France, 2018. arXiv:<https://telematics.poliba.it/publications/2018/GrassiICT2018.pdf>.
- [26] A. Grassi, G. Piro, G. Boggia, A look at Random Access for Machine-Type Communications in 5G cellular networks, Internet Technology Letters (2018).
- [27] S. Martiradonna, A. Grassi, G. Piro, L. A. Grieco, G. Boggia, An open source platform for exploring NB-IoT system performance, in: Proc. of IEEE European Wireless (EW), Catania, Italy, 2018. arXiv:<https://telematics.poliba.it/publications/2018/MartiradonnaEW2018.pdf>.
- [28] S. Martiradonna, G. Piro, G. Boggia, On the Evaluation of the NB-IoT Random Access Procedure in Monitoring Infrastructures, Sensors 19 (2019).
- [29] A. Grassi, G. Piro, G. Boggia, M. Kurras, W. Zirwas, R. SivaSiva Ganesan, K. Pedersen, L. Thiele, Massive MIMO Interference Coordination for 5G Broadband Access: Integration and System Level Study, Computer Networks (Elsevier) 147 (2018) 191–203. To be published, doi: 10.1016/j.comnet.2018.10.012.
- [30] E. Soltanmohammadi, K. Ghavami, M. Naraghi-Pour, A Survey of Traffic Issues in Machine-to-Machine Communications Over LTE, IEEE Internet of Things Journal 3 (2016) 865–884.
- [31] M. Lauridsen, L. C. Gimenez, I. Rodriguez, T. B. Sørensen, P. E. Mogensen, From LTE to 5G for Connected Mobility., IEEE Communications Magazine 55 (2017) 156–162.
- [32] M. S. Elbamby, C. Perfecto, M. Bennis, K. Doppler, Toward Low-Latency and Ultra-Reliable Virtual Reality, IEEE Network 32 (2018) 78–84.
- [33] E. Dahlman, G. Mildh, S. Parkvall, J. Peisa, J. Sachs, Y. Selén, J. Sköld, 5G wireless access: requirements and realization, IEEE Communications Magazine 52 (2014) 42–47.
- [34] D. Jiang, H. Wang, E. Malkamaki, E. Tuomaala, Principle and Performance of Semi-Persistent Scheduling for VoIP in LTE System, in: 2007 International Conference on Wireless Communications, Networking and Mobile Computing, IEEE, 2007, pp. 2861–2864.
- [35] E. Hossain, M. Rasti, H. Tabassum, A. Abdelnasser, Evolution toward 5G multi-tier cellular wireless networks: An interference management perspective, IEEE Wireless Communications 21 (2014) 118–127.
- [36] L. Lu, G. Y. Li, A. L. Swindlehurst, A. Ashikhmin, R. Zhang, An Overview of Massive MIMO: Benefits and Challenges, IEEE journal of selected topics in signal processing 8 (2014) 742–758.
- [37] L. Militano, M. Condoluci, G. Araniti, A. Molinaro, A. Iera, G.-M. Muntean, Single Frequency-Based Device-to-Device-Enhanced Video Delivery for Evolved Multimedia Broadcast and Multicast Services, IEEE Transactions on Broadcasting 61 (2015) 263–278.
- [38] G. Araniti, M. Condoluci, P. Scopelliti, A. Molinaro, A. Iera, Multicasting over emerging 5G networks: Challenges and perspectives, IEEE Network 31 (2017) 80–89.
- [39] J. J. Gimenez, D. Gomez-Barquero, J. Morgade, E. Stare, Wideband Broadcasting: A Power-Efficient Approach to 5G Broadcasting, IEEE Communications Magazine 56 (2018) 119–125.
- [40] S. Chen, J. Hu, Y. Shi, Y. Peng, J. Fang, R. Zhao, L. Zhao, Vehicle-to-everything (v2x) services supported by lte-based systems and 5g, IEEE Communications Standards Magazine 1 (2017) 70–76.
- [41] J. Harris, M. Beach, A. Nix, P. Thomas, The Potential of Offloading and Spectrum Sharing for 5G Vehicular Infotainment, in: 2016 IEEE

- 84th Vehicular Technology Conference (VTC-Fall), IEEE, 2016, pp. 1–5.
- [42] J. Wang, J. Liu, N. Kato, Networking and Communications in Autonomous Driving: A Survey, IEEE Communications Surveys & Tutorials 21 (2018) 1243–1274.
- [43] M. Boban, K. Manolakis, M. Ibrahim, S. Bazzi, W. Xu, Design aspects for 5G V2X physical layer, in: Standards for Communications and Networking (CSCN), 2016 IEEE Conference on, IEEE, 2016, pp. 1–7.
- [44] Patrik Cerwall, Ericsson Mobility Report - November, Technical Report, 2019.
- [45] A. Adhikary, X. Lin, Y.-P. E. Wang, Performance evaluation of nb-iot coverage, in: 2016 IEEE 84th Vehicular Technology Conference (VTC-Fall), IEEE, 2016, pp. 1–5.
- [46] C. Bockelmann, N. Pratas, H. Nikopour, K. Au, T. Svensson, C. Stefanovic, P. Popovski, A. Dekorsy, Massive machine-type communications in 5G: Physical and MAC-layer solutions, IEEE Communications Magazine 54 (2016) 59–65.
- [47] H. Holma, A. Toskala, T. Nakamura, 5G Technology: 3GPP New Radio, John Wiley & Sons, 2020.
- [48] 3GPP, 5G; NR; Base Station (BS) radio transmission and reception (Release 15), Technical Report 38104, 3rd Generation Partnership Project, 2018.
- [49] 3GPP, 5G; NR; Physical channels and modulation (Release 15), Technical Report 38211, 3rd Generation Partnership Project, 2020.
- [50] 3GPP, 5G; NR; Overall description (Release 15), Technical Report 38300, 3rd Generation Partnership Project, 2020.
- [51] K. Pedersen, G. Pocovi, J. Steiner, A. Maeder, Agile 5g scheduler for improved e2e performance and flexibility for different network implementations, IEEE Communications Magazine 56 (2018) 210–217.
- [52] T. Inoue, 5g nr release 16 and millimeter wave integrated access and backhaul, in: 2020 IEEE Radio and Wireless Symposium (RWS), IEEE, 2020, pp. 56–59.
- [53] 3GPP, Study on NR-based access to unlicensed spectrum (Release 16), Technical Report 38889, 3rd Generation Partnership Project, 2018.
- [54] Nokia, Key directions for Release 17, Technical Report RP-190831, 3rd Generation Partnership Project, 2019.
- [55] T. R. Henderson, M. Lacage, G. F. Riley, C. Dowell, J. Kopena, Network simulations with the ns-3 simulator, SIGCOMM demonstration 14 (2008) 527.
- [56] N. Baldo, M. Miozzo, M. Requena-Esteso, J. Nin-Guerrero, An open source product-oriented lte network simulator based on ns-3, in: Proceedings of the 14th ACM international conference on Modeling, analysis and simulation of wireless and mobile systems, ACM, 2011, pp. 293–298.
- [57] Y. Kim, J. Bae, J. Lim, E. Park, J. Baek, S. I. Han, C. Chu, Y. Han, 5g k-simulator: 5g system simulator for performance evaluation, in: 2018 IEEE International Symposium on Dynamic Spectrum Access Networks (DySPAN), 2018, pp. 1–2. doi:10.1109/DySPAN.2018.8610404.
- [58] S. Chen, S. Sun, Y. Wang, G. Xiao, R. Tamrakar, A comprehensive survey of TDD-based mobile communication systems from TD-SCDMA 3G to TD-LTE (A) 4G and 5G directions, China Communications 12 (2015) 40–60.
- [59] Arizona State University, Video Trace Library, 2019. URL: <http://trace.eas.asu.edu/>, [Online; Accessed 11 Sep. 2019].
- [60] R. Salami, C. Laflamme, B. Bessette, J.-P. Adoul, Description of itu-t recommendation g. 729 annex a: reduced complexity 8 kbit/s cs-acelp codec, in: 1997 IEEE International Conference on Acoustics, Speech, and Signal Processing, volume 2, IEEE, 1997, pp. 775–778.
- [61] J. Hoadley, P. Maveddat, Enabling small cell deployment with hetnet, IEEE Wireless Communications 19 (2012) 4–5.
- [62] A. Damjanovic, J. Montojo, Y. Wei, T. Ji, T. Luo, M. Vajapeyam, T. Yoo, O. Song, D. Malladi, A survey on 3GPP heterogeneous networks, IEEE Wireless communications 18 (2011) 10–21.
- [63] R. R. Roy, Handbook of mobile ad hoc networks for mobility models, volume 170, Springer, 2011.
- [64] 3GPP, 5G; NR; Physical layer procedures for data (Release 15), Technical Report 38214, 3rd Generation Partnership Project, 2018.
- [65] E. Tuomaala, H. Wang, Effective sinr approach of link to system mapping in ofdm/multi-carrier mobile network (2005).
- [66] C.-X. Wang, J. Bian, J. Sun, W. Zhang, M. Zhang, A Survey of 5G Channel Measurements and Models, IEEE Communications Surveys & Tutorials 20 (2018) 3142–3168.
- [67] I. Kostić, Analytical approach to performance analysis for channel subject to shadowing and fading, IEE Proceedings-Communications 152 (2005) 821–827.
- [68] ITU-R, Guidelines for Evaluation of Radio Interface Technologies for IMT-Advanced, Technical Report M.2135, 2008.
- [69] 3GPP, Study on 3D channel model for LTE, Technical Report 36873, 3rd Generation Partnership Project, 2015.
- [70] 3GPP, 5G; Study on channel model for frequencies from 0.5 to 100 GHz, Technical Report 38901, 3rd Generation Partnership Project, 2018.
- [71] A. Goldsmith, Wireless communications, Cambridge university press, 2005.
- [72] 3GPP, E-UTRA and E-UTRAN; LTE physical layer; Radio Frequency (RF) system scenarios (Release 14), Technical Report 36201, 3rd Generation Partnership Project, 2017.
- [73] 3GPP, Simulation assumptions and parameters for FDD HeNB RF requirements, Technical Report R4-092042, 3rd Generation Partnership Project, 2009.
- [74] Y. d. J. Bultitude, T. Rautiainen, IST-4-027756 WINNER II Channel Models, Technical Report D1.1.2 V1.2, 2008.
- [75] ITU-R, Guidelines for Evaluation of Radio Interface Technologies for IMT-2020, Technical Report M.2412, 2017.
- [76] X. He, K. Niu, Z. He, J. Lin, Link layer abstraction in mimo-ofdm system, in: 2007 International Workshop on Cross Layer Design, 2007, pp. 41–44. doi:10.1109/IWCLD.2007.4379036.
- [77] N. Nikaein, M. K. Marina, S. Manickam, A. Dawson, R. Knopp, C. Bonnet, OpenAirInterface: A flexible platform for 5G research, ACM SIGCOMM Computer Communication Review 44 (2014) 33–38.
- [78] I. Gomez-Migueluez, A. Garcia-Saavedra, P. D. Sutton, P. Serrano, C. Cano, D. J. Leith, srsLTE: an open-source platform for LTE evolution and experimentation, in: Proceedings of the Tenth ACM International Workshop on Wireless Network Testbeds, Experimental Evaluation, and Characterization, 2016, pp. 25–32.
- [79] Ericsson, Summary from email discussion on calibration step 1+2, Technical Report R1-092019, 3rd Generation Partnership Project, 2009.
- [80] Ericsson, Email discussion summary on calibration step 1c, Technical Report R1-092742, 3rd Generation Partnership Project, 2009.
- [81] 3GPP, Evolved Universal Terrestrial Radio Access (E-UTRA); Physical layer procedures (Release-10), Technical Report 36213, 3rd Gener-

- ation Partnership Project, 2010.
- [82] J. C. Ikuno, M. Wrulich, M. Rupp, Performance and modeling of LTE H-ARQ, in: International ITG Workshop on Smart Antennas WSA, 2009.
- [83] Free Software Foundation, Inc., The GNU Awk User's Guide, 2019. URL: <https://www.gnu.org/software/gawk/manual/gawk.html>, [Online; Accessed 30 Mar. 2020].
- [84] T. L. Marzetta, Noncooperative cellular wireless with unlimited numbers of base station antennas, IEEE Transactions on Wireless Communications 9 (2010) 3590–3600.
- [85] J. Nam, A. Adhikary, J.-Y. Ahn, G. Caire, Joint spatial division and multiplexing: Opportunistic beamforming, user grouping and simplified downlink scheduling, IEEE Journal of Selected Topics in Signal Processing 8 (2014) 876–890.
- [86] Z. Jiang, A. F. Molisch, G. Caire, Z. Niu, Achievable rates of fdd massive mimo systems with spatial channel correlation, IEEE Transactions on Wireless Communications 14 (2015) 2868–2882.
- [87] X. Rao, V. K. Lau, Distributed compressive csit estimation and feedback for fdd multi-user massive mimo systems, IEEE Transactions on Signal Processing 62 (2014) 3261–3271.
- [88] M. S. Sim, J. Park, C.-B. Chae, R. W. Heath, Compressed channel feedback for correlated massive mimo systems, Journal of Communications and Networks 18 (2016) 95–104.
- [89] J. Choi, D. J. Love, P. Bidigare, Downlink training techniques for fdd massive mimo systems: Open-loop and closed-loop training with memory, IEEE Journal of Selected Topics in Signal Processing 8 (2014) 802–814.
- [90] A. Adhikary, J. Nam, J.-Y. Ahn, G. Caire, Joint spatial division and multiplexing—the large-scale array regime, IEEE transactions on information theory 59 (2013) 6441–6463.
- [91] FANTASTIC-5G D2.1, Air interface framework and specification of system level simulations, Technical Report 2.1, 2016.
- [92] P. Marsch, Ö. Bulakci, O. Queseth, M. Boldi, 5G System Design: Architectural and Functional Considerations and Long Term Research, John Wiley & Sons, 2018.
- [93] L. Rong, O. B. Haddada, S.-E. Elayoubi, Analytical analysis of the coverage of a MBSFN OFDMA network, in: Global Telecommunications Conference, 2008. IEEE GLOBECOM 2008. IEEE, IEEE, 2008, pp. 1–5.
- [94] 3GPP, E-UTRA and E-UTRAN; Radio Resource Control (RRC); Protocol specification (Release 15), Technical Report 36331, 3rd Generation Partnership Project, 2018.
- [95] J. Kim, D. Munir, S. Hasan, M. Chung, Enhancement of LTE RACH through extended random access process, Electronics Letters 50 (2014) 1399–1400.
- [96] 3GPP, 5G; NR; Medium Access Control (MAC) protocol specification (Release 15), Technical Report 38321, 3rd Generation Partnership Project, 2018.
- [97] 3GPP, E-UTRA and E-UTRAN; LTE physical layer; General description (Release 15), Technical Report 36201, 3rd Generation Partnership Project, 2018.
- [98] 3GPP, E-UTRA and E-UTRAN; Overall description (Release 15), Technical Report 36300, 3rd Generation Partnership Project, 2018.
- [99] 3GPP, E-UTRA and E-UTRAN; Physical channels and modulation (Release 14), Technical Report 36211, 3rd Generation Partnership Project, 2017.
- [100] L. Zanzi, V. Sciancalepore, On Guaranteeing End-to-End Network Slice Latency Constraints in 5G Networks, in: Proc. IEEE International Symposium on Wireless Communication Systems (ISWCS), 2018.
- [101] M. Bennis, M. Debbah, H. V. Poor, Ultrareliable and Low-Latency Wireless Communication: Tail, Risk, and Scale, Proceedings of the IEEE 106 (2018) 1834–1853.
- [102] Y. Zeng, R. Zhang, T. J. Lim, Wireless communications with unmanned aerial vehicles: Opportunities and challenges, IEEE Communications Magazine 54 (2016) 36–42.
- [103] B. Li, Z. Fei, Y. Zhang, Uav communications for 5g and beyond: Recent advances and future trends, IEEE Internet of Things Journal 6 (2018) 2241–2263.
- [104] Y. Zeng, J. Lyu, R. Zhang, Cellular-connected uav: Potential, challenges, and promising technologies, IEEE Wireless Communications 26 (2018) 120–127.
- [105] A. A. Khuwaja, Y. Chen, N. Zhao, M.-S. Alouini, P. Dobbins, A survey of channel modeling for uav communications, IEEE Communications Surveys & Tutorials 20 (2018) 2804–2821.
- [106] 3GPP, 5G; NR; Study on NR Vehicle-to-Everything (V2X) (Release 16), Technical Report 38885, 3rd Generation Partnership Project, 2019.
- [107] R. I. Ansari, C. Chrysostomou, S. A. Hassan, M. Guizani, S. Mumtaz, J. Rodriguez, J. J. Rodrigues, 5g d2d networks: Techniques, challenges, and future prospects, IEEE Systems Journal 12 (2017) 3970–3984.
- [108] J. Garcia-Morales, M. C. Lucas-Estañ, J. Gozalvez, Latency-sensitive 5g ran slicing for industry 4.0, IEEE Access 7 (2019) 143139–143159.
- [109] 3GPP, Aspects; Management and orchestration; Concepts, use cases and requirements (Release 15), Technical Report 28530, 3rd Generation Partnership Project, 2018.
- [110] R. Su, D. Zhang, R. Venkatesan, Z. Gong, C. Li, F. Ding, F. Jiang, Z. Zhu, Resource allocation for network slicing in 5g telecommunication networks: A survey of principles and models, IEEE Network (2019).
- [111] P. Rost, C. Mannweiler, D. S. Michalopoulos, C. Sartori, V. Sciancalepore, N. Sastry, O. Holland, S. Tayade, B. Han, D. Bega, et al., Network slicing to enable scalability and flexibility in 5g mobile networks, IEEE Communications magazine 55 (2017) 72–79.
- [112] S. Rangan, T. S. Rappaport, E. Erkip, Millimeter wave cellular wireless networks: Potentials and challenges, arXiv preprint arXiv:1401.2560 (2014).



Sergio Martiradonna is a Ph.D. Student in Electrical and Information Engineering at Politecnico di Bari, Italy. He received a Double Degree in Internet Engineering from Politecnico di Bari, Italy, and from Université de Nice-Sophia-Antipolis, France, in 2017. Previously, he was a researcher with the CNIT (Italian University Consortium for Telecommunications). His research interests include 5G, 4G and NB-IoT networks, as well as system-level simulation tools. He is one of the main developer of 5G-air-simulator.



Alessandro Grassi received his Ph.D. degree in information engineering at “Politecnico di Bari”, Italy, in 2019. He received a first level degree in electronics engineering in 2012 and a second level degree (cum laude) in telecommunications engineering in 2015. His research interests include 4G and 5G cellular networks, scheduling and QoS optimization in wireless networks, broadcasting in cellular networks, MIMO and Massive MIMO techniques, and random access protocols for cellular machine-to-machine communications. He is a core developer of the 5G-air-simulator and he has been involved in the EU Horizon-2020 project “FANTASTIC-5G”.



Giuseppe Piro has been an Assistant Professor in Telecommunication at Politecnico di Bari since November 2018. In March 2018, he held the habilitation as “Associate Professor” in Telecommunications Engineering, according to the National Scientific Habilitation procedure (ASN 2016-2018). He received a first level degree and a second level degree (both cum laude) in Telecommunications Engineering from “Politecnico di Bari”, Italy, in 2006 and 2008, respectively. He received the Ph.D. degree in Electronic Engineering from “Politecnico di Bari”, Italy, on March 2012. His main research interests include secure Internet of Things and Industry 4.0, 5G systems, data-centric and programmable architectures for the Future Internet, nano-networks, Internet models and network measurements. His research activity is documented in more than 80 peer-reviewed international journals and conference papers, accounting for more than 3800 citations and a H-index of 24 (Scholar Google). At the time of this writing, he is the local investigator of the PRIN project no. 2017NS9FEY entitled “Realtime Control of 5G Wireless Networks: Taming the Complexity of Future Transmission and Computation Challenges”.

Moreover, he is involved in the European EU H2020 GUARD project. He is also involved in Italian MIUR PON projects (Pico&Pro, FURTHER, AGREED, RAFAEL) and in Apulia Region (Italy) Research project INTENTO. He founded 5G-ai-simulator, LTE-Sim, and NANO-SIM projects and is a developer of Network Simulator 3. In the past, he was involved in EU H2020 projects, like FANTASTIC-5G, BONVOYAGE, and symbIoTe, as well as in the “Apulia Israel joint Accelerator (AIJA)” project. He is also regularly involved as member of the TPC of many prestigious international conferences. Currently, he serves as Associate Editor for Sensors journal (MDPI), Internet Technology Letter (Wiley) and Wireless Communications and Mobile Computing journal (Hindawi).



Gennaro Boggia received, with honors, the Dr. Eng. and Ph.D. degrees in electronics engineering, both from the Politecnico di Bari, Bari, Italy, in July 1997 and March 2001, respectively. Since September 2002, he has been with the Department of Electrical and Information Engineering, Politecnico di Bari, where he is currently a Full Professor. From May 1999 to December 1999, he was a Visiting Researcher with the TILab, TelecomItalia Lab, Torino, Italy, where he was involved in the study of the core network for the evolution of Third-Generation (3G) cellular systems. In 2007, he was a Visiting Researcher at FTW, Vienna, Austria, where he was involved in activities on passive and active traffic monitoring in 3G networks. He has authored or coauthored more than 150 papers in international journals or conference proceedings, gaining more than 2300 citations. He is active in the IETF ICNRG working group and in the IEEE WG 6TiSCH. He is also regularly involved as a Member of the Technical Program Committee of many prestigious international conferences. His research interests include the fields of Wireless Networking, Cellular Communication, Internet of Things (IoT), Network Security, Security in IoT, Information Centric Networking (ICN), Protocol stacks for industrial applications, Internet measurements, and Network Performance Evaluation. Dr. Boggia is currently an Associate Editor for the IEEE Commun. Mag., the ETT Wiley Journal, and the Springer Wireless Networks journal.

Dr. Boggia is currently an Associate Editor for the IEEE Commun. Mag., the ETT Wiley Journal, and the Springer Wireless Networks journal.